

1 **Seasonal in situ observations of glyoxal and methylglyoxal**
2 **over the temperate oceans of the Southern Hemisphere**

3 **S.J. Lawson¹, P.W. Selleck¹, I.E. Galbally¹, M.D. Keywood¹, M.J. Harvey², C.**
4 **Lerot³, D. Helmig⁴, and Z. Ristovski⁵**

5 [1] {Commonwealth Scientific and Industrial Research Organisation, Oceans and
6 Atmosphere Flagship, Aspendale, Australia}

7 [2] {National Institute of Water and Atmospheric Research, Wellington, New Zealand}

8 [3] {Belgian Institute for Space Aeronomy, Brussels, Belgium}

9 [4] {Institute of Arctic and Alpine Research, University of Colorado, Boulder, USA}

10 [5]{International Laboratory for Air Quality & Health, Queensland University of
11 Technology, Brisbane, Australia.}

12 Correspondence to: S.J Lawson (sarah.lawson@csiro.au)

13

14 **Abstract**

15 Dicarbonyls glyoxal and methylglyoxal have been measured with 2,4-dinitrophenylhydrazine
16 (2,4-DNPH) cartridges and high performance liquid chromatography (HPLC), optimised for
17 dicarbonyl detection, in clean marine air over the temperate Southern Hemisphere (SH)
18 oceans. Measurements of a range of dicarbonyl precursors (volatile organic compounds,
19 VOCs) were made in parallel. These are the first in situ measurements of glyoxal and
20 methylglyoxal over the remote temperate oceans. Six 24 hour samples were collected in
21 summer (Feb-Mar) over the Chatham Rise in the South West Pacific Ocean during the
22 Surface Ocean Aerosol Production (SOAP) voyage in 2012, while 34 24 hour samples were
23 collected at Cape Grim Baseline Air Pollution Station in late winter (Aug-Sep) 2011.
24 Average glyoxal mixing ratios in clean marine air were 7 ppt at Cape Grim, and 23 ppt over
25 Chatham Rise. Average methylglyoxal mixing ratios in clean marine air were 28 ppt at Cape
26 Grim and 10 ppt over Chatham Rise. The mixing ratios of glyoxal at Cape Grim are the
27 lowest observed over the remote oceans, while mixing ratios over Chatham Rise are in good
28 agreement with other temperate and tropical observations, including concurrent MAX-DOAS
29 observations. Methylglyoxal mixing ratios at both sites are comparable to the only other

1 marine methylglyoxal observations available over the tropical Northern Hemisphere (NH)
2 ocean. Ratios of glyoxal : methylglyoxal > 1 over Chatham Rise but <1 at Cape Grim,
3 suggest different formation and/or loss processes or rates dominate at each site. Dicarbonyl
4 precursor VOCs, including isoprene and monoterpenes, are used to calculate an upper
5 estimate yield of glyoxal and methylglyoxal in the remote marine boundary layer and explain
6 at most 1-3 ppt of dicarbonyls observed, corresponding to 10% and 17% of the observed
7 glyoxal and 29% and 10% of the methylglyoxal at Chatham Rise and Cape Grim,
8 respectively, highlighting a significant but as yet unknown production mechanism. Surface –
9 level glyoxal observations from both sites were converted to vertical columns and compared
10 to average vertical column densities (VCDs) from GOME-2 satellite retrievals. Both satellite
11 columns and in situ observations are higher in summer than winter, however satellite vertical
12 column densities exceeded the surface observations by more than 1.5×10^{14} molecules cm⁻² at
13 both sites. This discrepancy may be due to the incorrect assumption that all glyoxal observed
14 by satellite is within the boundary layer, or may be due to challenges retrieving low VCDs of
15 glyoxal over the oceans due to interferences by liquid water absorption, or use of an
16 inappropriate normalisation reference value in the retrieval algorithm. This study provides
17 much needed data to verify the presence of these short lived gases over the remote ocean and
18 provide further evidence of an as yet unidentified source of both glyoxal and also
19 methylglyoxal over the remote oceans.

20 **1 Introduction**

21 Natural aerosols, including sea spray and secondary aerosols originating from marine
22 dimethyl sulphide (DMS), have been shown to strongly affect the uncertainty of cloud
23 radiative forcing in global climate models, highlighting a need to understand the composition
24 and microphysical properties of marine aerosol in very pristine marine environments
25 (Carslaw et al., 2013). While primary emissions, including wind-blown sea salt, make a large
26 contribution to aerosol mass in the remote marine boundary layer (MBL), organic carbon can
27 make a significant contribution to the mass of submicron marine aerosol in the more
28 biologically active summer months (O'Dowd et al., 2004; Facchini et al., 2008a; Sciare et al.,
29 2009; Ovadnevaite et al., 2011b). This organic carbon may be primary organic matter,
30 including polymer microgels, viruses, bacteria, colloids and organic detritus, directly
31 transferred from bulk water and the sea surface microlayer (SML) of the ocean to the
32 atmosphere during bubble burst (Orellana et al., 2011; Facchini et al., 2008b). The organic
33 carbon may also comprise secondary aerosol, formed from oxidation of gas phase ocean-

1 derived volatile organic compounds (VOCs) such as DMS, isoprene and monoterpenes (Shaw
2 et al., 2010).

3 The organic component of marine aerosol is chemically complex and requires multiple state
4 of the art techniques to elucidate (Fu et al., 2013; Fu et al., 2011; Decesari et al., 2011;
5 Rinaldi et al., 2010; Claeys et al., 2010). A further challenge is the more recent blurring of
6 distinction between primary and secondary organics, in which oxidative ageing and
7 evaporation of semi volatile primary organic aerosol (POA) leads to production of gas phase,
8 volatile, low molecular weight products, which may then go to form secondary organic
9 aerosol (SOA) (Donahue et al., 2014). The resulting photochemically processed POA may
10 have similar chemical properties to, and is sometimes loosely classified as SOA. (Rinaldi et
11 al., 2010; Decesari et al., 2011; Ovadnevaite et al., 2011b). This interrelatedness of primary
12 and secondary organics adds considerable complexity to understanding the formation and
13 chemical processing of organic aerosols in the MBL.

14 The influence of organics on cloud condensation nuclei (CCN) activity of marine aerosol in
15 general appears to be highly variable and investigations have mostly focused on primary
16 organic aerosol (Ovadnevaite et al., 2011a; Meskhidze et al., 2011; Orellana et al., 2011;
17 Westervelt et al., 2012; Topping et al., 2013). The contribution of DMS oxidation products
18 to the CCN population over the remote Southern Ocean has been well established (Korhonen
19 et al., 2008; Ayers and Gras, 1991), however an understanding of the contribution of other
20 secondary aerosol species such as isoprene and monoterpene derived-SOA to the CCN
21 activity of marine aerosol is still emerging. Meskhidze and Nenes et al. (2006) suggested a
22 link between isoprene-derived SOA over a phytoplankton bloom site and cloud
23 microphysical and radiative properties in the Southern Ocean, while Lana et al. (2012) found
24 a correlation between modelled secondary sulphur and organic aerosols and variability of
25 cloud microphysics derived from satellite observations over the remote mid and high latitude
26 ocean.

27 The alpha dicarbonyl glyoxal (CHOCHO) is an important SOA aerosol precursor which in
28 recent years has found to be widespread in the marine boundary layer (MBL), both via
29 column measurements (Lerot et al., 2010; Vrekoussis et al., 2009; Mahajan et al., 2014;
30 Wittrock et al., 2006) and in situ measurements (Coburn et al., 2014). The dominant source of
31 glyoxal is oxidation of parent VOCs, with isoprene globally the most important precursor
32 (explaining 47% of glyoxal formation) (Fu et al., 2008). Glyoxal has a global average
33 lifetime of about 3 hours (Fu et al., 2008; Myriokefalitakis et al., 2008; Stavrakou et al.,

1 2009), and is highly water soluble and so can diffuse into aerosol or cloud water where it is
2 converted to SOA through formation of low volatility products such as organic acids and
3 oligimers (Ervens et al., 2011; Kampf et al., 2013; Sedehi et al., 2013; Lee et al., 2011; Lim
4 et al., 2013). Alpha dicarbonyl methylglyoxal (CHOCCH_3O), a close relative of glyoxal, also
5 forms low volatility products in the aqueous phase (Tan et al., 2012; Sedehi et al., 2013; Lim
6 et al., 2013), has a short global lifetime of 1.6 hours and is produced by oxidation of gas
7 phase parent compounds, predominantly isoprene (Fu et al., 2008). Destruction of both
8 dicarbonyls is mainly via photolysis, followed by reaction with OH (Myriokefalitakis et al.,
9 2008, Fu et al., 2008). The global sources of glyoxal and methylglyoxal are significant (45 Tg
10 C a^{-1} and 140 Tg a^{-1} globally), and their SOA yield, which occurs mainly in clouds, is
11 comparable in magnitude to SOA formation from other oxidation products of biogenic VOCs
12 and aromatics (Fu et al., 2008). Major oxidation products of glyoxal and methylglyoxal at in-
13 cloud relevant concentrations are oxalic and pyruvic acids (Lim et al., 2013).

14 There is considerable evidence that the dicarbonyls, and particularly glyoxal, makes an
15 important contribution to the organic component of marine aerosol over the remote oceans.
16 Both dicarbonyls have been found in marine aerosols over the Atlantic Ocean (van Pinxteren
17 and Herrmann, 2013) and Pacific Oceans (Bikkina et al., 2014), with dicarbonyl mass
18 positively correlated to organic acids (including oxalic acid) and ocean biological activity.
19 Oxalic acid has been consistently found in pristine marine aerosol from remote sites
20 including Amsterdam Island (Claeys et al., 2010), Mace Head (Rinaldi et al., 2010), Cape
21 Verde (Muller et al., 2010) and Cape Grim (unpublished data), with highest concentrations
22 during the biologically active summer months, coinciding with maximum concentrations of
23 DMS oxidation products methanesulfonic acid (MSA) and non-sea-salt sulphate. Rinaldi et
24 al. (2011) reported that oxalic acid in submicron marine aerosol from Mace Head and
25 Amsterdam Island showed a similar seasonal cycle to SCIAMACHY glyoxal columns, and a
26 chemical box model was able to explain the observed oxalate using the glyoxal columns.

27 However, significant unknowns remain. There are currently insufficient methylglyoxal
28 observations to confirm its presence and importance to SOA formation over the remote
29 oceans, and understanding the source of the observed glyoxal in the MBL has proven
30 challenging. If the production of glyoxal is indeed due only to oxidation of precursor VOCs,
31 calculating the expected yield of glyoxal should be straightforward in this relatively simple
32 and well mixed chemical matrix over the remote ocean. However, there has been consistent
33 suggestion that glyoxal concentrations in the MBL are in excess of the yields expected from

1 its precursors. Wittrock et al. (2006) reported enhanced concentrations of formaldehyde and
2 glyoxal from SCIAMACHY satellite retrievals over tropical oceans, but were unable to
3 reproduce observations using a global model. More detailed global modelling studies by Fu et
4 al. (2008) and Myriokefalitakis et al. (2008) were also unable to reproduce SCIAMACHY
5 glyoxal column retrievals over the tropical oceans, highlighting the possibility of unknown
6 biogenic marine sources. Later satellite retrievals of glyoxal from SCIAMACHY (Vrekoussis
7 et al., 2009), GOME-2 (Lerot et al., 2010) and recently from OMI (Miller et al., 2014) have
8 provided further evidence of the widespread presence and seasonal modulation of glyoxal
9 over biologically active oceans, although in some regions, such as the temperate SH oceans,
10 the columns are close to satellite detection limits.

11 Glyoxal and methylglyoxal were first observed in the atmosphere and seawater in the
12 Caribbean and Sargasso Seas as early as 1989 (Zhou and Mopper, 1990) where
13 concentrations of glyoxal and methylglyoxal in seawater were 4 and 2 orders of magnitude
14 too low to explain the atmospheric concentrations. MAX-DOAS retrievals observed hundreds
15 of ppt glyoxal in the Gulf of Maine (Sinreich et al., 2007) and an average of 63 ppt glyoxal
16 over the remote Tropical Pacific (Sinreich et al., 2010). The Sinreich et al. (2010)
17 measurements were sufficiently far from land that the glyoxal observed was either from
18 unrealistically high mixing ratios of long lived terrestrial precursors, or more likely a
19 substantial unknown source possibly of marine origin, in support of earlier modelling and
20 satellite studies. The widespread presence of glyoxal over the remote oceans was recently
21 confirmed by Mahajan et al. (2014), who reported MAX-DOAS and long-path DOAS
22 differential slant column densities from 10 field campaigns in both hemispheres in tropical
23 and temperate regions. A global average value of about 25 ppt was reported with an upper
24 limit of 40 ppt, however over the Southern Hemisphere oceans, particularly in sub tropical
25 and temperate regions, glyoxal mixing ratios were mostly below instrument detection limits.

26 In 2014 an additional source of glyoxal in the MBL was identified in laboratory studies
27 (Zhou et al., 2014), when oxidation of the sea surface microlayer (SML) led to emission of
28 low molecular weight oxygenated compounds including glyoxal. However, the atmospheric
29 yields of glyoxal were low, attributed to the fast irreversible hydrolysis of glyoxal which
30 prevents transfer of glyoxal to the atmosphere. Van Pinxteren and Herrmann (2013) observed
31 a glyoxal enrichment factor of 4 in SML compared to the bulk ocean, but the concentration
32 observed was several orders of magnitude too low to explain mixing ratios of 10s of ppt
33 typically seen in the MBL (Sinreich et al., 2010). The first eddy-covariance flux

1 measurements of glyoxal were recently made over the oceans, using an in situ Fast Light
2 Emitting Diode Cavity Enhanced Differential Optical Absorption Spectroscopy (LED-CE-
3 DOAS instrument) (Coburn et al., 2014). Negative flux (glyoxal transfer into the ocean) was
4 observed in both hemispheres during the day, and a positive flux from the ocean in the SH at
5 night. However, despite this first evidence of a direct oceanic source of glyoxal to the
6 atmosphere, the positive flux at night could explain only 4 ppt of the glyoxal observed in the
7 overlying atmosphere (some 30 % of the overnight increase), implying the contribution of
8 another night-time production mechanism.

9 Despite these recent advances in our understanding of glyoxal production processes, our
10 current inability to reconcile the presence of these short lived gases over the remote ocean
11 suggests we have not identified a significant source of glyoxal. It is likely that this
12 unidentified source also contributes to the glyoxal production in polluted terrestrial
13 environments, but is masked by a large contribution from anthropogenic precursors such as
14 acetylene. The production of glyoxal from photochemical processing of organic aerosol is a
15 possible contributor (Vrekoussis et al., 2009; Stavrakou et al., 2009; Bates et al., 2012)
16 though this remains unconfirmed. An additional source may be entrainment of glyoxal and its
17 precursors from the free troposphere into the MBL, particularly in light of recent observations
18 of non-negligible mixing ratios of glyoxal in the free troposphere (Volkamer, 2014).

19 A more in depth understanding is currently hindered by a lack of dicarbonyl observations in
20 the MBL. While recent studies have contributed substantial additional observations of
21 glyoxal over the remote oceans (Coburn et al., 2014; Mahajan et al., 2014), there have been
22 no studies which have made parallel measurements of gas phase precursors, and so expected
23 yields of glyoxal are only estimates. No in situ observations of glyoxal have been reported
24 over temperate oceans of either hemisphere, and there is only one previous study reporting
25 methylglyoxal observations over the world's oceans (in the tropical northern hemisphere,
26 NH) (Zhou and Mopper, 1990). With the exception of the Caribbean and Sargasso Sea
27 measurements (Zhou and Mopper, 1990), all column and in situ observations of glyoxal over
28 the remote oceans have used optical measurement techniques (Mahajan et al., 2014; Sinreich
29 et al., 2010; Sinreich et al., 2007; Coburn et al., 2014). Finally, given the challenges in
30 retrieving low VCDs of glyoxal over the ocean from satellite observations (Lerot et al., 2010;
31 Vrekoussis et al., 2009; Miller et al., 2014), more ground based measurements are required.

32 We provide much needed in situ glyoxal and methylglyoxal data from the very sparsely
33 measured temperate oceans of the Southern Hemisphere. Observations have been made using

1 derivatisation of dicarbonyls on 2-4 DNPH cartridges and analysis with HPLC, which is an
2 alternative measurement technique to the optical techniques used widely for oceanic glyoxal
3 observations to date. Measurements have been made in two seasons, summer and winter, and
4 auxiliary measurements, including carbon dioxide, radon and particles have been used to
5 conclusively remove the possibility of any terrestrial influence on the dicarbonyl
6 observations. This is the first study to concurrently measure a range of dicarbonyl precursors
7 (VOCs), so that the yield of dicarbonyls from its gas phase precursors can be conclusively
8 determined. Finally we provide the first methylglyoxal observations over the temperate
9 remote ocean.

10

11 **2 Methods**

12 **2.1 Sampling locations**

13 Dicarbonyl in situ observations were made at the Cape Grim Baseline Air Pollution Station
14 (CGBAPS) and during a voyage over the Chatham Rise in the South West Pacific Ocean
15 during the Surface Ocean Aerosol Production (SOAP) study (see Fig. 1).

16 **2.1.1 Cape Grim Baseline Air Pollution Station**

17 The Cape Grim Baseline Air Pollution Station (BAPS) is located on the north-west tip of the
18 island state of Tasmania, Australia, (40.683°S 144.689°E). CGBAPS is a World
19 Meteorological Organisation (WMO) Global Atmosphere Watch (GAW) Global Station and
20 hosts a wide variety of long term measurements including greenhouse gases, ozone depleting
21 substances, aerosols, radon and reactive gases. The station is situated on a cliff 94m above
22 sea level and when the wind blows from the south westerly ‘Baseline’ sector the air that
23 arrives at the station has travelled over the Southern Ocean several days prior with no
24 terrestrial influence (see Sec. 2.2.2.)

25 A total of 33 samples were collected from the 26 August – 29 September in 2011 (late
26 winter-early spring). Each 24 hour sample consisted of approximately 2000L of air drawn
27 through a 2,4-DNPH S10 Cartridge (Supelco) at a flow rate of 1.8L min⁻¹.

28 Ambient air was sampled down a 150mm diameter stainless steel inlet stack which extends
29 10m above the roof deck and is 104m above sea level. The flow rate of the intake was
30 235 L min⁻¹ to ensure laminar flow was maintained. The DNPH cartridges were loaded in a

1 custom designed ‘Sequencer’ which allows up to 16 cartridges to be automatically sampled
2 for a predefined time and sequence. The Sequencer drew air via a 3m length of $\frac{1}{4}$ inch PFA
3 tubing which was extended into the centre of the stainless steel intake stack. Samples were
4 collected in all wind directions and an ozone scrubber (KI impregnated filter) was placed in
5 front of the cartridges. Chlorophyll-*a*, a measure of ocean biological activity, is low in the
6 Southern Ocean in winter, with typical values of $0.1\text{--}0.2\text{ mg m}^{-3}$ (Bowie et al., 2011). Air
7 temperatures throughout the sampling period ranged from 7°C - 13°C with an average of 10°C
8 and total rainfall during the sample period at the station was 90 mm. The average relative
9 humidity was 78%.

10 Data collected from concurrent and continuous carbon dioxide, particle count and radon
11 measurements at Cape Grim have been included in this work as indicators for clean marine
12 air (see Sec. 2.2.2). VOC data from canister samples collected at Cape Grim for the NOAA
13 Halocarbon (HATS) group and the Carbon Cycle Network have been used to calculate
14 dicarbonyl yields (see Sec. 2.2.3)

15 2.1.2 Surface Ocean Aerosol Production (SOAP) voyage

16 The SOLAS-endorsed Surface Ocean Aerosol Production Study in 2012 investigated links
17 between ocean biogeochemistry, air-sea exchange of trace gases and particles, and the
18 composition of the overlying atmosphere (Landwehr et al., 2014). Measurements were made
19 on board the RV Tangaroa over Chatham Rise, located over the biologically productive
20 subtropical oceanic front. Six dicarbonyl samples were collected from the 29th Feb- 6th
21 March 2012 (late summer). Each 24 hour sample consisted of approximately 1400L of air
22 drawn through a 2,4 DNPH S10 Cartridge (Supelco) at a flow rate of 1.3 L min^{-1} . Cartridges
23 were loaded in the “Sequencer” which drew air off a 25m 3/8 inch PFA inlet line with a flow
24 rate of 10 L min^{-1} . Inlet losses were determined to be <2% for isoprene, monoterpenes,
25 methanol and dimethyl sulphide however losses were not specifically tested for dicarbonyls
26 due to the absence of a gaseous calibration standard. The sample inlet line pulled air from the
27 crow’s nest of the vessel above the bridge, some 28 m above sea level. To avoid ship exhaust
28 from aft of the inlet being drawn into the PFA inlet line and sampled on to the cartridges, a
29 baseline switch was developed and deployed using a CR3000 micrologger control system
30 (Campbell Scientific, Logan UH). The switch used 1 Hz wind data from the vessel
31 port/starboard pair of Wind Observer anemometers (Gill Instruments, Lymington, U.K.) and
32 was configured to switch pumps off within 1 second of detecting non-baseline conditions.

1 The “baseline” was defined as: a five second running average relative windspeed $> 3 \text{ ms}^{-1}$
2 and 5 second vector averaged relative wind direction outside of the aft (135° to 225° relative
3 degrees) wind-direction with meteorological convention of 0° at the bow. Five minute
4 duration under accepted windspeed and direction was required before turning on. During
5 experimentation and for much of the “steaming” transit legs, the vessel was oriented into the
6 wind for as much of the time as possible in addition to dedicated periods of steaming into the
7 wind. This resulted in a high frequency (~75%) of baseline conditions throughout the
8 voyage.

9 During the voyage three distinct phytoplankton blooms were sampled, and dicarbonyl
10 samples reported in this work were taken over the third bloom during the last 6 days of the
11 voyage. Underway chlorophyll- α during this period ranged between $0.3\text{-}0.9 \text{ mg m}^{-3}$ ($10^{\text{th}}\text{-}90^{\text{th}}$
12 percentile) with median of 0.5 mg m^{-3} (calibrated against discrete data with data
13 corresponding to sky irradiance $>50\text{W/m}^2$ removed, i.e. to exclude daytime data affected by
14 photo-quenching). The bloom consisted of a mixed phytoplankton population of
15 coccolithophores, small flagellates and dinoflagellates, and had a deep cold mixed layer
16 characteristic of Sub-Antarctic waters. During the 6 days of sampling the vessel moved
17 between 44.928°S and 41.261°S and 172.768°E to 175.168°E , including transiting to Lyttelton
18 Port on the East Coast of the New Zealand South Island for several hours on the 1st March to
19 exchange staff. However due to south westerly winds during this period and high wind
20 speeds (average of 13 ms^{-1} and max of 29 ms^{-1}), air was predominantly of marine origin. Air
21 temperatures during the sampling period ranged from 10°C - 18°C with an average of 13°C
22 and total rainfall during the 6 day sample period was 3.0 mm. The average relative humidity
23 was 80% during the voyage.

24 Parallel measurements also made during the SOAP voyage which have been utilised in this
25 work, include online VOCs via Proton Transfer Reaction Mass Spectrometry (PTR-MS) (see
26 Sec. 2.2.3) and carbon dioxide and particle concentrations (Sec. 2.2.2).

27 **2.2 In situ measurements**

28 **2.2.1 DNPH cartridges and HPLC analysis**

29 During sampling, carbonyls and dicarbonyls were trapped on S10 Supelco cartridges,
30 containing high purity silica adsorbent coated with 2,4-dinitrophenylhydrazine (2,4-DNPH),
31 where they are converted to the hydrazone derivatives. Samples were refrigerated

1 immediately after sampling until analysis. The derivatives were extracted from the cartridge
2 in 2.5 ml of acetonitrile and analysed by a High Performance Liquid Chromatography
3 (HPLC) system consisting of a Dionex GP40 gradient pump, a Waters 717 autosampler, a
4 Shimadzu System controller SCL-10A VP, a Shimadzu diode array detector (DAD) SPD-
5 M10A VP, a Shimadzu Column Oven CTO-10AS VP and Shimadzu CLASS-VP
6 chromatography software. The compound separation was performed with two Supelco
7 Supelcosil LC-18 columns in series, 5 μ m, 4.6 mm ID x 250 mm in length, Part No 58298.
8 The chromatographic conditions include a flow rate of 1.6 ml min⁻¹ and an injection volume
9 of 25 μ l, and the DAD was operated in the 220nm to 520nm wavelength range. The peaks
10 were separated by gradient elution with an initial mobile phase of 64% acetonitrile and 36%
11 deionised water for 10 minutes, then a linear gradient to 100% acetonitrile at 20 min, and
12 column temperature of 30°C. The deionised water used for analysis was 18.2 M Ω .cm grade
13 produced from a Millipore Milli-Q Advantage 10 system and HPLC grade acetonitrile was
14 purchased from Merck.

15 Standards for glyoxal and methylglyoxal were prepared by making hydrazone crystals from
16 glyoxal (40% wt in H₂O), methylglyoxal (40% wt in H₂O) and derivatisation reagent
17 2,4,DNPH (all from Sigma-Aldrich). The crystals were weighed and dissolved in acetonitrile
18 to produce a stock standard for the glyoxal and methylglyoxal derivatives, which was used to
19 make up a range of standards from 0.125 to 1.000 μ g ml⁻¹ which gave a linear response with
20 a correlation coefficient of 0.999 for both derivatives.

21 The DAD enables the absorption spectra of each peak to be determined. The mono carbonyl
22 DNPH derivatives all have a similar shaped absorption spectrum with a maximum absorption
23 near 360nm. In contrast, the dicarbonyls glyoxal and methylglyoxal have absorption spectra
24 which differ in shape to the monocarbonyls, and have a maximum absorption near 435nm
25 (Fig. 2). The difference in the spectra highlights which peaks in the chromatograms are
26 mono- or dicarbonyl DNPH derivatives and along with retention times allows identification
27 of the glyoxal and methylglyoxal peaks. Quantifying the dicarbonyl DNPH derivatives at
28 435nm results in increased peak height and also has the added benefit of reducing the peak
29 area of any co-eluting mono-carbonyl DNPH derivatives (Fig. 3). All samples, blanks and
30 standards for glyoxal and methylglyoxal in this work were quantified using absorption at 435
31 nm which as discussed above is optimised for dicarbonyl detection.

32 Sample recovery was determined by spiking 1 μ g of glyoxal and methylglyoxal on to DNPH
33 cartridges – recoveries were 96 \pm 0.3 % for glyoxal and 111 \pm 8 % for methylglyoxal. The

1 degree of derivatisation was examined in these spiked cartridges to ensure both carbonyl
2 groups in the glyoxal and methylglyoxal molecules had reacted with the 2-4, DNPH (Wang et
3 al., 2009; Olsen et al., 2007). Analysis of samples that had been extracted within the last 24
4 hours showed a second smaller peak indicating that ~ 5% of the glyoxal had reacted to form
5 mono-derivatives rather than bis-derivatives (e.g. only one carbonyl group had reacted).
6 However analysis of samples that were held for > 24 hours after extraction showed all of the
7 mono derivative had been converted into the bis-derivative. As all samples were extracted
8 then held for at least 24 hours before analysis, complete derivatisation to the bis-derivative is
9 expected. For methylglyoxal there was no evidence of any mono-derivatives. The total mass
10 of carbonyls and dicarbonyls sampled on the DNPH cartridges was at most 7% of the
11 cartridge capacity, and collection efficiencies of >93% have been determined for carbonyls
12 on DNPH cartridges at similar flow rates to those used here (Zhang et al., 1994; Slemr,
13 1991; Grutter et al., 2005). Hence no significant losses of dicarbonyls during sampling are
14 expected.

15 The minimum detectable limit (MDL) for glyoxal and methylglyoxal were calculated from
16 the standard deviation of field blanks collected during the study period based on the
17 principles of ISO 6879 (ISO, 1995). Field blanks were opened and installed in the Sequencer
18 sampling train for the same time period as samples. MDLs for a 24 hour sample were 1 ppt
19 (glyoxal) and 1.7 ppt (methylglyoxal) during SOAP, and 0.6 ppt (glyoxal) and 0.9 ppt
20 (methylglyoxal) at Cape Grim. Glyoxal and methylglyoxal mixing ratios were above MDLs
21 in all 24 hour samples.

22 2.2.2 Supporting measurements for selection of clean marine periods

23 HYSPLIT (<https://ready.arl.noaa.gov/HYSPLIT.php>) 96 hour air-mass back trajectories
24 (300m above sea level) were used as an additional means of identifying clean marine samples
25 from Cape Grim and the Chatham Rise (see Figs. 4a and 4b). Specific surface measurements
26 used to indicate clean marine air for each site are discussed below.

27 Cape Grim

28 Atmospheric radon-222, carbon dioxide and particle concentration data were used to select
29 dicarbonyl samples with clean marine origin and no terrestrial influence.

30 Atmospheric radon-222 is a useful atmospheric tracer to determine the degree of contact
31 between an air parcel and a terrestrial surface, due to the much larger flux of radon from

1 terrestrial surfaces compared with the ocean. Hourly atmospheric radon-222 measurements at
2 Cape Grim are made on air taken from a 70 inlet (height above sea level 164 m) and using the
3 dual-flow loop two filter method. See Zahorowski et al. (2013) for details of the measurement
4 technique and application of radon data to identify clean marine air.

5 Carbon dioxide (CO_2) concentrations may be used to indicate whether an air mass is
6 primarily of marine origin or has had recent contact with land. Terrestrial contact results in
7 enhancement or draw down of CO_2 depending on the land use and anthropogenic sources.
8 Continuous CO_2 measurements at Cape Grim are sampled via a 70m inlet and measured via a
9 continuous, ultra precise CSIRO LOFLO NDIR system, described elsewhere (Steele et al.,
10 2014). Hourly averaged CO_2 concentrations were used in this work.

11 Particle concentration may be used as an indicator of an air mass history, as recent contact
12 with a terrestrial surface leads to particle concentrations enhanced above low concentrations
13 typically found in marine air. Measurements of condensation (CN) nuclei greater than 10 nm
14 in diameter ($\text{CN} > 10 \text{ nm}$) are made at Cape Grim using a 3010 CPC TSI particle counter,
15 sampling from the 10 m sample inlet described in Sec 2.1.1 (Gras, 2009). Hourly averaged
16 particle concentration data was used in this work.

17 Baseline status at Cape Grim

18 Air is automatically classified as Baseline at Cape Grim (e.g. clean marine air) using a
19 combination of wind direction (190° and 280°) and a seasonally adjusted particle
20 concentration ($\text{CN} > 10 \text{ nm}$) threshold based upon the previous five year's particle
21 concentration data (Keywood, 2007). This Baseline status was used to identify clean marine
22 samples.

23 SOAP Voyage

24 Carbon dioxide and particle concentrations ($\text{CN} > 10 \text{ nm}$) were used to identify dicarbonyl
25 samples with a clean marine origin and no terrestrial influence during the voyage.

26 Carbon dioxide (CO_2) measurements were made continuously using a Picarro Cavity
27 Ringdown laser (CRDS). The instrument was calibrated before and during the voyage using
28 three reference calibration tanks. The CO_2 intake through 6 mm Decabon tubing, from
29 alongside the crow's nest had a flow rate of 300 mL min^{-1} .

30 $\text{CN} > 10 \text{ nm}$ concentrations were measured with a 3010 CPC TSI particle counter. Antistatic
31 (copper coil) polyurethane ducting was used as a common aerosol inlet, and sampled air from

1 the main radar tower at 21 m in height above sea level. The inlet was 10 cm in diameter, 30 m
2 in length, with a flow rate of 800 L m^{-1} . The CPC intake was connected to the common
3 aerosol inlet via $\frac{1}{4}$ inch stainless steel tubing. Inlet loss tests indicated particle loss rates were
4 $\sim 15\%$ for total particle counts.

5

6 2.2.3 Measurements for dicarbonyl yield calculations

7 A High Sensitivity Proton Transfer Reaction-Mass Spectrometer (PTR-MS) (Ionicon
8 Analytik) was used to measure VOCs in real time during the SOAP voyage. Details on PTR-
9 MS measurements are given in Galbally et al. (2007) and some additional information is
10 provided here.

11 The PTR-MS ran with inlet and drift tube temperature of 60°C , 600V drift tube, ~ 2.2 mbar
12 drift tube pressure, which equates to an energy field of 133 Td. The O_2^+ signal was $<1\%$ of
13 the primary ion H_3O^+ signal. The PTR-MS sampled from a 25 m PFA 3/8 inch inlet line,
14 which had a continuous flow of 10 L min^{-1} , except during ‘non baseline’ periods when the
15 inlet pump switched off and the PTR-MS sampled room air through a VOC scrubber. The
16 Baseline status was logged on two separate programs and PCs and so room air measurements
17 were removed from the data. The PTR-MS measured in scan mode in the range of m/z 21 –
18 m/z 155 with a dwell time of 10 seconds per mass, allowing 3 full scans of the mass range per
19 hour. Measurement of background signal resulting from interference ions and outgassing of
20 materials was achieved by passing ambient air through Platinum coated glass wool catalyst at
21 350°C for 30 minutes 4 times per day. An interpolated background signal was used for
22 background correction. All species used in this work were calibrated daily by introducing a
23 known flow of calibration gas to VOC-free ambient air which had previously passed through
24 the catalyst. Calibrations and background measurements were carried out using an automated
25 calibration system, see Galbally et al. (2007). Calibration gases used were $\sim 1 \text{ ppm}$ custom
26 VOC mixture in nitrogen Apel Riemer ($\sim 1 \text{ ppm}$ acetone, benzene, toluene, m-xylene, a-
27 pinene) and a custom gas mixture from Scott Specialty Gases ($\sim 1 \text{ ppm}$ isoprene and 1,8-
28 cineole).

29 The MDL for a single 10 s measurement of a selected mass was determined using the
30 principles of ISO6879 (ISO, 1995) i.e. 5% of the 10 s background measurements give a
31 false positive reading. MDLs were as follows: m/z 59 (acetone) 17 ppt, m/z 69 (isoprene) 28
32 ppt, m/z 79 (benzene) 16 ppt, m/z 93 (toluene) 16 ppt, m/z 107 (sum xylenes) 19 ppt, m/z 137

1 (sum monoterpenes) 66 ppt. In contrast to the first week of the voyage, the mixing ratios of
2 VOCs during the last 6 days of the voyage were low and subsequently many of the VOCs
3 were below detection limit. The percentage of observations above MDL during this period
4 are as follows m/z 59 – (95%), m/z 69- (14%), m/z 79- (15%), m/z 93- (14%), m/z 107 –
5 (7%), m/z 137-(4%). Where the observation was lower than MDL, the half MDL value was
6 substituted. Hence due to the high periods of time that VOCs were below MDLs, the reported
7 concentrations used for yield calculation are strongly influenced by the MDL. Reported
8 mixing ratios of dicarbonyl precursors and dicarbonyl yields calculated with PTR-MS data
9 (Sec. 2.5) are therefore likely to be an upper limit.

10

11 VOC Flask data

12 VOCs measurements from flasks collected at Cape Grim in Baseline conditions were used to
13 provide supplementary mixing ratios for species which were not targeted, or could not be
14 measured with sufficient sensitivity by PTR-MS at Cape Grim and during the SOAP voyage.

15 Stainless steel and glass flasks have been collected for and analysed by the National Oceanic
16 Atmospheric Administration (NOAA) Earth System Research Laboratory (ESRL) Global
17 Monitoring Division (GMD) Halocarbons (HATS) group with Gas Chromatography (GC)
18 techniques since the early 1990s (Montzka et al., 2014). In this work, benzene and acetylene
19 mixing ratios (analysed with GC-mass spectrometry detection (Rhoderick et al., 2014; Pétron
20 et al., 2012)) from August- September 2011 were utilised, as well as acetylene values in
21 March 2011, as a proxy for mixing ratios during SOAP. Benzene values are calculated from
22 an average of 6 pairs of flasks (2 glass and 4 stainless steel pairs) while acetylene values are
23 from 3 pairs of stainless steel flasks in Aug-Sep 2011 and a single pair of stainless steel flasks
24 in March 2011. There is low interannual variability in benzene and acetylene at Cape Grim,
25 so the values used, which correspond to the same sample periods as dicarbonyls, were
26 representative of typical values for these months.

27 Glass flasks collected in Baseline Air at Cape Grim for the NOAA Carbon Cycle Group are
28 analyzed for VOCs by an automated gas chromatography system at the University of
29 Colorado's Institute of Arctic and Alpine Research (INSTAAR) (Helmig et al., 2014;
30 Helmig et al., 2009). Average propane, iso-butane, n-butane, iso-pentane, and n-pentane
31 mixing ratios were utilised from 5 pairs of glass flasks collected in Aug-Sep 2011 (filtered
32 data). Flask data were also used to estimate alkane mixing ratios during the SOAP voyage

1 (average mixing ratios from flasks sampled in March between 2005-2014). The following
2 number of flasks were used in calculating average values for March: propane (4 pairs and 2
3 single flasks), n-butane (9 pairs and 4 single flasks), iso-butane (10 pairs and 2 single flasks),
4 n-pentane (7 pairs and 2 single flasks) and iso-pentane (10 pairs and 2 single flasks).

5 Additional VOC measurements from Cape Grim were utilised for the dicarbonyl yield
6 calculations, including online PTR-MS measurements in clean air at Cape Grim in February
7 (summer) 2006 (Galbally et al., 2007), online PTR-MS measurements in clean air in spring
8 (November) 2007 (Lawson et al., 2011), in which data has been further filtered to include
9 only Baseline hours (Sec. 2.2.2) and stainless steel canisters which were collected at Cape
10 Grim between 1998 – 2000 and analysed at Aspendale with GC with flame ionisation
11 detection (FID) (Kivlighon, 2001). Further details of how these data were utilised is provided
12 in Sec. 3.3 and Table 3.

13 OH and ozone concentrations

14 Precursor (VOC) lifetimes at Chatham Rise and Cape Grim were calculated using estimated
15 OH concentrations, and measured ozone mixing ratios from Cape Grim in March and August
16 –September respectively.

17 [OH] was estimated from a simple steady state chemical model where:



20 OH is presumed to be removed overwhelmingly by reaction with carbon monoxide and
21 methane (Sommariva et al., 2004). $J(O^1D)$ is estimated from UV-B measurements for 2000 –
22 2005 inclusive (Wilson, 2014). All other chemical parameters are measured at Cape Grim
23 (hourly averages) except for ozone where climatological values were used. The full
24 temperature dependence of reaction rates was used.

25 Average measured ozone mixing ratios in Baseline air at Cape Grim were taken from Molloy
26 et al. (2014).

27

1 **3 Results and Discussion**

2 **3.1 In situ observations in clean marine air**

3 **3.1.1 Selection of clean marine samples**

4 Five of the 33 samples from Cape Grim, and 2 of the 6 samples from Chatham Rise were
5 identified as coming from a clean marine back trajectory air over the 24 hour sampling
6 period. Mixing ratios of glyoxal and methylglyoxal at Cape Grim and Chatham Rise in clean
7 marine air alongside supporting measurements are shown in Table 1. Air mass back
8 trajectories (96 hour) for these clean marine samples are shown in Figs. 4a and 4b.

9 Samples were identified as being of clean marine origin in the following way. Samples from
10 Cape Grim were initially identified as those for which > 90% of the sample hours were
11 classified as Baseline according to the criteria described in Sec. 2.2.2. Between 92-97% of
12 the sampling time was Baseline for the clean marine samples. Chatham Rise clean marine
13 samples were initially identified using the HYSPLIT air mass back trajectories, and in situ
14 measured wind direction. As an additional indicator of clean marine baseline air, concurrent
15 measurements of in situ continuous CO₂, and CN > 10nm were calculated for Cape Grim and
16 SOAP samples (see Table 1). Concurrent atmospheric radon-222 concentrations were also
17 calculated for Cape Grim samples.

18 The pristine marine nature of these samples is clearly demonstrated by these supporting
19 measurements. The particle concentration (CN>10nm) at Cape Grim during sampling of
20 clean marine samples was 194 particles cm⁻³, lower than the typical concentration of ~400
21 particles cm⁻³ in Baseline air in August/September (Gras, 2014). Particle concentrations
22 corresponding to the Chatham Rise clean marine samples are also low (328 particles cm⁻³)
23 but with a large standard deviation of 1591 particles cm⁻³. This is due to short-lived, major
24 enhancements (up to 30,000 particles cm⁻³) of CN, which correspond to measured
25 enhancements in black carbon, identifying ship exhaust. This raises the possibility that there
26 may have been a minor influence of ship exhaust on the VOC measurements, even though the
27 VOC and aerosol inlets were not co-located. While glyoxal and methylglyoxal have been
28 identified in medium duty diesel exhaust (Schauer et al., 1999), and so could be emitted by
29 the ship's diesel engine, Schauer et al. (1999) showed that oxygenated VOCs such as
30 acetaldehyde and acetone were present in mixing ratios 10-20 times higher than glyoxal. No

1 coincident spike in acetaldehyde or other VOCs were seen with the particle peaks – therefore
2 it is unlikely that ship exhaust had any influence on the glyoxal or methylglyoxal measured.

3 Average CO₂ concentrations during clean marine samples were 388.84 (std dev 0.12) and
4 388.54 ppm (std dev 0.8) at Cape Grim and SOAP respectively, very close to Southern Ocean
5 Baseline concentrations in August 2011 (388.51 ppm) and March 2012 (388.69 ppm)
6 (<http://www.csiro.au/greenhouse-gases/>). The higher standard deviation from Chatham Rise
7 was due to positive CO₂ excursions above background and is therefore likely also a minor
8 impact of ship exhaust.

9 Finally the atmospheric radon-222 concentration of 43 mBq m⁻³ at Cape Grim is indicative of
10 clean marine air. This value compares well to a median baseline sector value of 42 mBq m⁻³
11 and is much lower than the median non-baseline value of 378 mBq m⁻³ reported by
12 Zahorowski et al (2013).

13 3.1.2 Dicarbonyl observations in clean marine air

14 The glyoxal mixing ratio at Cape Grim in winter is low (7 ± 2 ppt), and in contrast is higher
15 over Chatham Rise in summer (23 ± 8 ppt). The low standard deviations indicate consistency
16 in glyoxal mixing ratios in clean marine air at both sites. The higher mixing ratios in summer
17 compared to winter are in agreement with higher VCDs of glyoxal in summer compared to
18 winter over the temperate SH oceans as observed by SCIAMACHY and GOME-2
19 (Vrekoussis et al., 2009; Lerot et al., 2010) (see Sec. 3.4 for further discussion of satellite
20 comparison).

21 In contrast to glyoxal, the methylglyoxal mixing ratios in pristine marine air are higher at
22 Cape Grim (28 ± 11 ppt) compared to Chatham Rise (10 ± 10 ppt). The average ratio of
23 glyoxal:methylglyoxal in clean marine air is ~4 over Chatham rise (range 1.7-5.9) while at
24 Cape Grim the average ratio is 0.3 (range 0.2-0.4) Given that many of the gas phase
25 precursors of methylglyoxal are also precursors of glyoxal this major difference in ratios at
26 the two sites is striking, and is also seen when taking into account non-pristine marine
27 samples. Possible reasons for this difference are discussed in Sec. 3.2.3 below.

28 3.2 Clean marine versus all data and comparison with other marine 29 background observations

30 Cape Grim and Chatham Rise dicarbonyl observations from clean marine samples and for all
31 samples are presented in Table 2. For comparison, other studies reporting mixing ratios of

1 glyoxal and methylglyoxal from remote temperate and tropical oceans are also presented.
2 Where other studies have explicitly excluded possibility of terrestrial influence via back
3 trajectories or other means, these values are listed as 'clean marine.' Where possibility of
4 terrestrial influence has not been investigated, values are listed as 'all data', however values
5 listed under 'all data' are not necessarily affected by air of terrestrial origin.

6 3.2.1 Glyoxal

7 Average mixing ratios of glyoxal at both Cape Grim and Chatham Rise are higher when
8 averaging all samples (which include air from all wind directions and hence terrestrial
9 sources), compared to clean marine samples. This is expected as the terrestrial environment is
10 a major source of important biogenic dicarbonyl precursor gases isoprene and alpha-pinene,
11 and is also a source of precursors from anthropogenic and biomass burning sources, including
12 longer lived gases such as acetylene, benzene, acetone, alkanes and $>C_2$ alkenes which can
13 travel long distances before being oxidised. Higher standard deviations in all samples
14 compared to clean marine samples likely reflects a greater variation in concentrations of
15 precursor gases resulting from differing wind directions. Interestingly, at Cape Grim, the
16 average enhancement in glyoxal when including data from all wind direction is only 3 ppt,
17 even though a further 28 samples have been included. This suggests terrestrial sources have a
18 minimal contribution to glyoxal mixing ratios at Cape Grim in winter.

19 The glyoxal mixing ratio from Cape Grim of 7 ppt in clean marine conditions and 10 ppt in
20 all conditions, is the lowest mixing ratio that has been reported over the world's oceans to
21 date. This low mixing ratio is supported in part by the study by Mahajan et al. (2014), in
22 which many of the observations over the temperate SH oceans were below detection limits.
23 The glyoxal mixing ratio from Chatham Rise all data (30 ± 12 ppt) compares well to the
24 mixing ratio derived from MAX- DOAS measurements during the same voyage (23 ± 10 ppt)
25 (Mahajan et al., 2014). Despite the techniques employing different approaches (in situ
26 derivatised samples versus column measurement) this suggests good agreement between
27 these techniques at these low mixing ratios. Recent inter-comparisons of dicarbonyl
28 measurement techniques have examined the relationship between optical and derivatisation
29 techniques, but with a focus on a wider range of mixing ratios than observed over the remote
30 ocean (Thalman et al., 2014; Pang et al., 2014).

31 The glyoxal mixing ratios from Chatham Rise also compare well to those observed by
32 Mahajan et al. (2014) over the North Pacific and Atlantic (25 ± 13 ppt) and tropical Pacific

1 and Atlantic (24 ± 12 ppt SH, 26 ± 15 ppt NH). It should be noted that these Mahajan et al.
2 (2014) values were calculated only from data above the instrument detection limit and so
3 contain a positive bias and are upper estimates. Chatham Rise mixing ratios are also similar
4 to the Eastern Tropical Pacific NH average (32 ± 6 ppt) (Coburn et al., 2014) but somewhat
5 lower than those observed in the SH Eastern Tropical Pacific (43 ± 9 ppt) (Coburn et al.,
6 2014), and over the Tropical Pacific (63 ± 21 ppt) (Sinreich et al., 2010). The Caribbean Sea
7 value of 80 ppt is the highest average mixing ratio reported over the oceans and substantially
8 higher than mixing ratios observed in this study, although the variation of this value is not
9 given (Zhou and Mopper, 1990). Overall, the synthesis of glyoxal observations from this and
10 other studies provides compelling evidence for the widespread presence of glyoxal, in non-
11 negligible mixing ratios, in the atmosphere over the remote oceans.

12 3.2.2 Methylglyoxal

13 Mixing ratios of methylglyoxal at Cape Grim and Chatham Rise are higher when considering
14 all data, and have greater variation, reflecting substantial influence of terrestrial precursors. In
15 particular, mixing ratios of methylglyoxal at Cape Grim in all samples are approximately
16 twice the mixing ratios of clean marine samples. This significant enhancement at Cape Grim
17 in all data is likely due to substantial terrestrial influence at Cape Grim when considering all
18 wind directions. The station is bounded by farmland to the east and south-east, and mainland
19 Australia, and the city of Melbourne is \sim 300km north across Bass Straight. The greater
20 enhancement of methylglyoxal compared to glyoxal in all data from Cape Grim may be due
21 to the much higher yield of methylglyoxal from isoprene and monoterpenes compared to
22 glyoxal, and the rich source of methylglyoxal precursors from urban regions including
23 alkenes and alkanes $> C_2$ (Fu et al., 2008).

24 The only other observations of methylglyoxal over the world's oceans come from the
25 Caribbean Sea (Zhou and Mopper, 1990), with an approximate value of ~ 10 ppt which is
26 somewhat lower than that observed at Cape Grim, but in agreement with Chatham Rise
27 mixing ratios in this study.

28 3.2.3 Differences between dicarbonyl ratios at Cape Grim and Chatham Rise

29 The average ratio of glyoxal: methylglyoxal is 3.8 over Chatham Rise (range 1.7-5.9) in clean
30 marine air and 2.3 in all samples (range 1.2-5.9). At Cape Grim the average ratio is 0.3 (range
31 0.2-0.4) in clean marine air and 0.2 in all samples (range 0.1-0.4). The dominance of

1 methylglyoxal at Cape Grim and glyoxal at Chatham Rise points to a major difference
2 between sites and warrants further investigation.

3 The back trajectories of air in clean marine samples at both Cape Grim and Chatham Rise
4 indicate that the air sampled at both sites originated from the Southern Ocean, from a latitude
5 of 55 - 65°S 96 hours prior (Fig. 4a and b). A major difference between the back trajectories
6 of the two sites is the longitude, with Cape Grim back trajectories covering 50 °E - 140°E and
7 the trajectories from the more easterly located Chatham Rise covering 90° E - 175°E. The 3-D
8 trajectory altitude (not shown), suggests that air from all clean oceanic samples at both sites
9 travelled in the lower 750m of troposphere 24 hours prior, and which up to 48 hours prior had
10 originated at a height of between 500-1500m (Chatham Rise) and 300-1200m (Cape Grim).
11 No clear differences in vertical back trajectories between sites, or relationship between height
12 and mixing ratios were evident.

13 Because glyoxal and methylglyoxal are so short lived, their observed mixing ratios are due to
14 equilibrium between local production and loss. Therefore the difference in ratios between
15 sites indicates a major difference or differences in production or loss rates.

16 If differences in ratios are due to differing rates of production of dicarbonyls, this could be
17 due to a) varying concentrations of precursor gases, b) different emission rates of dicarbonyls
18 from the SML, or c) other unconfirmed production mechanisms. Methylglyoxal and glyoxal
19 have a number of overlapping gas phase precursors, and while there are precursors specific to
20 each (e.g. acetylene, acetone and benzene for glyoxal and higher alkanes and alkenes for
21 methylglyoxal) (Fu et al., 2008), in clean marine conditions precursor mixing ratios are
22 unlikely to differ significantly between sites. The calculated yield of dicarbonyls from
23 parallel or best estimate precursor mixing ratios at both sites is low (see Sec. 3.3) and so other
24 production mechanisms must be dominating at these sites.

25 Emission of glyoxal from the SML has only very recently been reported for the first time
26 (Zhou et al., 2014), and there is no evidence as yet of direct emission of methylglyoxal from
27 the oceans. It is likely that methylglyoxal is emitted from the oceans: it has been measured
28 alongside glyoxal in the SML in concentrations which are enhanced above the bulk water,
29 indicating its production in the SML, (van Pinxteren and Herrmann, 2013; Zhou and Mopper,
30 1990). However, the relative abundance of methylglyoxal in the SML compared to glyoxal is
31 highly uncertain, but the studies that have investigated this have found higher concentrations
32 of glyoxal compared to methylglyoxal by a factor of 3 (van Pinxteren and Herrmann, 2013)

1 and 5 (Zhou and Mopper, 1990). Meanwhile, a laboratory study which detected glyoxal from
2 oxidation of the SML did not find evidence for methylglyoxal production (Zhou et al., 2014).
3 It is therefore possible that the ratio of glyoxal:methylglyoxal is higher at Chatham Rise
4 compared to Cape Grim due to enhanced direct emission of glyoxal from biologically
5 productive waters which were targeted over Chatham Rise, in contrast to Cape Grim which in
6 winter samples air which has passed over waters of low biological productivity. The
7 likelihood of SML as a major source of glyoxal is uncertain given the modest atmospheric
8 yields of glyoxal in laboratory studies (Zhou et al., 2014) and modest positive fluxes of
9 glyoxal from the tropical ocean (Coburn et al., 2014). However emission of dicarbonyls from
10 the temperate oceans has not been studied and so the temperate SML, as a source of
11 dicarbonyls particularly in biologically active regions such as Chatham Rise, cannot be
12 discounted.

13 It is also possible that the difference in dicarbonyl ratios between the two sites is due in part
14 to differences in loss rates between glyoxal and methylglyoxal. The major sink for both
15 dicarbonyls is photolysis which is unlikely to explain the difference in observed ratios. Other
16 sinks include oxidation by OH, irreversible uptake into cloud droplets and particles followed
17 by conversion to SOA, or wet or dry deposition (Fu et al., 2008). Satellite imagery shows
18 both sites had partial cloud cover during the sampling periods, however a major difference
19 was the amount of rainfall that occurred at Cape Grim (90 mm over 33 days) compared to
20 during dicarbonyl sampling on over Chatham Rise (3 mm over 6 days). Specifically during
21 sampling of the Cape Grim clean marine samples, 1-7 mm of rain fell each day, (sum 14.0
22 mm for 5 samples), while during clean marine Chatham Rise samples 0-0.4mm fell each day
23 (sum 0.57mm for 2 samples). It is possible that due to the higher Henry's law constant of
24 glyoxal compared to methylglyoxal (Kroll et al., 2005; Zhou and Mopper, 1990; Betterton
25 and Hoffmann, 1988), glyoxal was more efficiently removed from the atmosphere via wet
26 deposition at Cape Grim due to its more rapid uptake into aqueous particles. While wet
27 deposition is a globally minor sink, it is likely to be important at night in the absence of other
28 major sinks (Fu et al., 2008). However, the reason for this difference cannot conclusively be
29 determined. The only other observations of glyoxal and methylglyoxal over the open ocean
30 for comparison are in the tropics (Zhou and Mopper, 1990) and show an average glyoxal
31 mixing ratio far in excess of methylglyoxal mixing ratio. This is in direct contrast to Cape
32 Grim, and in partial agreement with the Chatham Rise results. Production and loss processes
33 at each site could be explored with chemical modelling.

1 **3.3 Calculation of expected glyoxal, methylglyoxal yields from measured**
2 **VOC precursors in clean marine air**

3 Expected yields of glyoxal and methylglyoxal were calculated, based, where possible, on
4 parallel precursor VOC measurements over Chatham Rise and Cape Grim (Table 3). Where a
5 concurrent measurement of a precursor was not available, an estimate was made. All
6 estimated precursor mixing ratios are identified, and the source of the estimate is given in
7 Table 3. Where no observations of the precursor at the site were available (e.g. toluene and
8 xylene in winter at Cape Grim), but observations of a similar compound class were available
9 (e.g. benzene) the mixing ratio of benzene was used as a reliable upper estimate for shorter-
10 lived toluene and xylenes. Where no observations of the precursor were available, and no
11 measurements of compounds from a similar class were available, mixing ratios were based on
12 the same precursor species at a different site (e.g. summer Cape Grim acetylene, alkene and
13 alkane observations were used for Chatham Rise). In other cases, in-situ observations from
14 the site in the same season were used, but based on measurements several years prior (e.g.
15 Cape Grim ethene and propene). Where observations from the specific season were not
16 available, e.g. winter isoprene, acetone and monoterpenes at Cape Grim, a spring or summer
17 value was used, which for isoprene and monoterpenes are likely to be an upper estimate.
18 Three dicarbonyl precursors, glycoaldehyde, methyl butenol and hydroxyacetone, were
19 excluded from the calculation as all are emitted from terrestrial processes (biomass burning
20 and biogenic emission) and are short-lived, so are unlikely to contribute to dicarbonyl
21 production over the remote ocean.

22 The expected mixing ratios of dicarbonyls that could be explained by oxidation of each
23 precursor were calculated according to the following equation:

$$24 \quad MR_{dicarbonyl} = \frac{MR_{precursor} \times Y_{dicarbonyl}}{\tau_{precursor}} \times \tau_{dicarbonyl} \quad (3)$$

25 Where $MR_{dicarbonyl}$ is mixing ratio of dicarbonyl, $MR_{precursor}$ is mixing ratio of precursor,
26 $Y_{dicarbonyl}$ = yield of dicarbonyl, τ_{prec} = lifetime of precursor and $\tau_{dicarbonyl}$ = lifetime of
27 dicarbonyl.

28 Global annual mean molar yields of glyoxal and methylglyoxal from precursor gases were
29 taken from Fu et al. (2008). Lifetimes of all precursors were calculated based on average
30 daytime concentrations of $[OH]$ of 8.7×10^5 molecules cm^{-3} at Chatham Rise in March and
31 3.7×10^5 molecules cm^{-3} at Cape Grim in August-September, except for monoterpenes (proxy

1 for alpha-pinene), isoprene and propene lifetimes which were based on the [OH] stated above
2 and [ozone] of 4.9×10^{11} molecules cm^{-3} at Chatham Rise and 8.0×10^{11} molecules cm^{-3} at
3 Cape Grim (see Sect 2.2.3). Global average lifetimes of glyoxal (2.9 hours) and
4 methylglyoxal (1.6 hours) were used (Fu et al., 2008).

5 Table 3. shows that the small proportion of glyoxal and methylglyoxal production accounted
6 for is largely driven by isoprene and monoterpenes. The precursors can explain at most 1-3
7 ppt of glyoxal and methylglyoxal at these two sites, which equates to only 17% and 10% of
8 glyoxal and 10% and 29% of methylglyoxal over Cape Grim and Chatham Rise, respectively.
9 By dividing the difference between the measured and calculated mixing ratios by the average
10 global lifetime of glyoxal and methylglyoxal, the production rate in the boundary layer
11 required to reconcile the measured and calculated dicarbonyl mixing ratios can be
12 determined. For glyoxal, the additional production rate required is 48 ppt/day (97 ppt C/day)
13 and 172 ppt/day (343 ppt C/day) while for methylglyoxal the additional production rate
14 required is 378 ppt/day (1135 ppt C/day) and 106 ppt/day (318 ppt C/day) at Cape Grim and
15 Chatham Rise.

16 As mentioned in Sec. 2.2.3, the isoprene and monoterpene mixing ratios over Chatham Rise
17 were below the instrument detection much of the time, and substitution of half MDLs may
18 result in an upper estimate of mixing ratios for these species. Regardless, this is the first study
19 which has used concurrent measurements of these important precursors to constrain the yields
20 of glyoxal and methylglyoxal. As parallel isoprene and monoterpene mixing ratios were not
21 available at Cape Grim the yield calculation used summer and spring isoprene and
22 monoterpene mixing ratios which are likely to result in an upper estimate of dicarbonyl
23 mixing ratios resulting from precursor oxidation. Conversely using the global average
24 lifetimes of glyoxal and methylglyoxal is likely to lead to an underestimate of the mixing
25 ratio of dicarbonyls at Cape Grim, as actual dicarbonyl lifetimes in winter at Cape Grim are
26 likely to be longer than the global average. The calculation also does not take into account
27 diurnal variation in production and loss rates. However, Coburn et al. (2014) showed that
28 while glyoxal over the Eastern Tropical Pacific varied by approximately 15 ppt (~30%)
29 between night and day, it did not decrease below 30 ppt at night (average both hemispheres).
30 The approach used here should therefore give a good approximation of the 24 hour
31 dicarbonyl mixing ratio expected from oxidation of precursors. The absence of photolytic
32 destruction and OH oxidation of dicarbonyls at night (the dominant known sinks), coupled
33 with an absence of dicarbonyl production through OH oxidation of precursors at night (the

1 dominant known source) likely contributes to the relatively constant mixing ratios between
2 day and night.

3 The low proportion of dicarbonyl mixing ratios that can be explained by oxidation of
4 precursors calculated here supports previous claims that there is unlikely to be sufficient
5 levels of VOC precursors over the remote oceans to explain the non-negligible levels of
6 glyoxal observed (Coburn et al., 2014; Sinreich et al., 2010). For the first time, we show that
7 the same applies to methylglyoxal over the ocean.

8 The large proportion of glyoxal and methylglyoxal which cannot be explained by the
9 precursor mixing ratios confirms the importance of other production mechanisms. As
10 discussed previously, it is unclear whether positive SML fluxes are sufficiently large to
11 explain the unaccounted for portion of these gases at Cape Grim and Chatham Rise. Kwan et
12 al (2006) estimated that OH oxidation of organic aerosol (OA) may result in a production rate
13 of up to 70 ppt C/day of OVOCs in the FT and a production rate of up to ~500 ppt C/day
14 OVOCs in the lower continental troposphere in the summertime. The combined boundary
15 layer production rate of glyoxal and methylglyoxal at Chatham Rise needed to reconcile the
16 measured and calculated mixing ratios is 661 ppt C/day, in reasonable agreement with the
17 Kwan et al (2006) estimate, while the Cape Grim glyoxal and methylglyoxal flux (1232 ppt
18 C/day) is a factor of 2-3 times higher. Whilst the Kwan et al (2006) estimates contained
19 significant uncertainties, and used continental measurements, they do suggest that oxidation
20 of OA may make a non-negligible contribution to the dicarbonyl mixing ratios.

21 Another possible production mechanism is oxidation of as yet unidentified gas phase
22 precursors.

23 **3.4 Comparison of glyoxal surface observations with satellite vertical
24 columns**

25 In situ glyoxal mixing ratios from Cape Grim and Chatham Rise were converted into vertical
26 column densities (VCDs) and compared with glyoxal VCDs from GOME-2 on Metop-A.

27 Mixing ratios were converted to VCDs assuming that all glyoxal observed was well mixed
28 within the boundary layer, and assuming standard conditions throughout the boundary layer
29 of temperature (25°C) and pressure (1 atm). Boundary layer heights of 850m were used for
30 both Chatham Rise (average of daytime and nocturnal radiosonde flights) and an average
31 modelled value for Cape Grim in all wind directions (unpublished data, see Zahorowski et al.

1 2013 for model details). Chatham Rise surface observations were compared to an average
2 GOME-2 column for March 2012 in the region 40-50 S and 170-180°E, while Cape Grim
3 surface observations were compared to GOME-2 columns taken from August-September
4 2011 in the region 39-42°S and 143-147°E.

5 In the Austral summer, GOME-2 glyoxal columns over the temperate oceans in the SH are
6 low, but somewhat higher than other remote regions, while in winter the columns are among
7 the lowest observed globally (Lerot et al., 2010). There is low inter-annual variability in the
8 GOME-2 glyoxal VCDs at both the regions encompassing Cape Grim and Chatham Rise, but
9 a clear seasonal cycle, with a maximum VCD in the summer months (Dec- Feb) and a
10 minimum in the autumn-winter months (May-August). The 2007-2012 average seasonal
11 variability of GOME-2 glyoxal VCDs from the sites above is shown in Figure 5. In June,
12 VCDs cannot be calculated due to insufficient satellite sensitivity resulting from observation
13 geometry (low angle of the sun).

14 Cape Grim VCDs calculated from in situ observations are 2.1×10^{13} molecules cm^{-2}
15 (standard error of mean 2.1×10^{12}), while Chatham Rise calculated VCDs are 6.3×10^{13}
16 molecules cm^{-2} (standard error of mean 1.0×10^{13}). In comparison, satellite retrieved VCDs
17 are 1.8×10^{14} molecules cm^{-2} for the Cape Grim region and 2.4×10^{14} molecules cm^{-2} for the
18 Chatham Rise region (both with an uncertainty of $\pm 1.3 \times 10^{14}$ molecules cm^{-2}) (Figure 5).
19 While both satellite columns and in situ columns observe higher VCD over Chatham Rise in
20 summer than Cape Grim in winter, the satellite VCDs exceed in situ VCDs at both sites by
21 $>1.5 \times 10^{14}$ molecules cm^{-2} . There are several possible factors that may be contributing to the
22 higher satellite VCD. The first reason may be due to the assumption that all of the glyoxal
23 observed by the satellites is in the boundary layer. Aircraft measurements made as part of the
24 TORERO campaign (Tropical Ocean Troposphere Exchange of Reactive Halogens and
25 OVCs), have confirmed the widespread presence of glyoxal in the free troposphere
26 (Volkamer, 2014). If glyoxal is also present in the free troposphere over the temperate SH
27 oceans, the satellite, which is sensitive to the entire troposphere, would indeed observe
28 glyoxal VCD larger than VCD calculated from in situ measurements, which represent only
29 the boundary layer. If glyoxal is widespread in the free troposphere this clearly has important
30 implications for the interpretation of satellite column data. Another reason may be due to the
31 significant challenges in retrieving low VCDs of glyoxal over the oceans, due to interferences
32 by liquid water absorption, discussed elsewhere (Vrekoussis et al., 2009; Lerot et al., 2010).
33 Also, the satellite glyoxal retrieval algorithm includes a normalization procedure comparing

1 actual retrieved columns to a reference value taken in a reference sector. As discussed in
2 Miller et al. (2014), this reference value might be too large. Another possible reason is that
3 the satellite VCDs are measured only once per day during the satellite overpass at 9:45am,
4 whereas the in situ observations reported here are 24 hour averages. If there is a diurnal
5 variation in glyoxal mixing ratios at these sites, as was shown over the Tropical Pacific
6 Ocean (Coburn et al., 2014), the satellite VCD may not be representative of the 24 hour
7 average.

8 Difficulty reconciling satellite VCDs and in situ observations over the ocean has recently
9 been noted elsewhere, including the tendency of satellite VCDs to exceed in situ
10 measurements, particularly in regions with low VCDs which are at the limits of satellite
11 sensitivity (Coburn et al., 2014; Mahajan et al., 2014). Further comparisons between in situ
12 and satellite observations over the oceans are needed, including characterisation of the
13 vertical distribution of glyoxal.

14 **4 Conclusions**

15 This work confirms the presence of short lived dicarbonyl glyoxal over the remote temperate
16 oceans, even in winter in very pristine air over biologically unproductive waters. We provide
17 the first observations of methylglyoxal over temperate oceans and confirm its presence
18 alongside glyoxal. These observations support the likely widespread contribution from these
19 dicarbonyls to SOA formation over the ocean.

20 Glyoxal mixing ratios at Cape Grim in winter are the lowest measured over the ocean, while
21 glyoxal at Chatham Rise is similar to other temperate mixing ratios, and similar to or at the
22 lower end of tropical observations. Methylglyoxal observations at Cape Grim and Chatham
23 Rise are comparable to the only other observations available (tropical Northern Hemisphere
24 ocean).

25 Chatham Rise glyoxal observations from this study agree well with observations made via
26 MAX-DOAS on the same voyage, suggesting a good agreement between the technique used
27 in this work (DNPH derivatisation with HPLC analysis optimised for dicarbonyl detection)
28 and the optical technique.

29 Different ratios of glyoxal: methylglyoxal were observed at the two locations, with an
30 average ratio in clean marine air of ~4 over Chatham Rise (range 1.7-5.9) and 0.3 at Cape
31 Grim (range 0.2-0.4). The reasons for this are unexplained but may be due to a larger positive
32 flux of glyoxal from biologically active waters over Chatham Rise, and/or to preferential loss

1 of glyoxal over methylglyoxal by wet deposition at Cape Grim. Chemical modelling is
2 suggested to better constrain the production and loss mechanisms.

3 Expected yields of glyoxal and methylglyoxal were calculated based on parallel
4 measurements of precursor VOCs, including isoprene and monoterpenes. At most, 1-3 ppt of
5 the glyoxal and methylglyoxal observed in clean marine air can be explained from oxidation
6 of these precursors, confirming a significant contribution from another source over the ocean.
7 While the SML has recently been confirmed as a direct source of glyoxal both in the field and
8 in laboratory studies, it seems unlikely this positive flux is a sufficiently large to explain the
9 atmospheric concentrations observed. Other possible, but unconfirmed sources may include
10 oxidation of as-yet unidentified gas precursors, or atmospheric oxidation of organic aerosol.

11 Glyoxal observations were converted to VCDs and compared with GOME-2 satellite VCDs.
12 While in situ and satellite observations both observe a higher glyoxal VCD in summer, the
13 satellite VCD exceeds the surface observations by more than 1.5×10^{14} molecules cm^{-2} .
14 Recent observations of glyoxal in the free troposphere suggest that this discrepancy is least in
15 part due to the incorrect assumption that all glyoxal observed over the ocean by satellites is in
16 the MBL. Other reasons for the discrepancy may be due to challenges in retrieving low
17 VCDs of glyoxal over the oceans, including accounting for interference by liquid water
18 absorption and selection of an appropriate normalisation reference value in the retrieval
19 algorithm. Further comparisons are needed, including characterisation of the vertical
20 distribution of glyoxal.

21 **Acknowledgements**

22 We thank Rob Gillett and Min Cheng (CSIRO), Nigel Somerville, Jeremy Ward and Sam
23 Cleland (Cape Grim BAPS) and Nick Talbot (NIWA) for assistance with sampling and
24 analysis and James Harnwell (CSIRO) for design and construction of Sequencer sampling
25 unit. We thank Cliff Law for excellent leadership during SOAP voyage and officers and crew
26 of R.V. Tangaroa and NIWA Vessels for logistics support.

27 Radon data and boundary layer heights courtesy of Alastair Williams, Scott Chambers and
28 Alan Griffiths (ANSTO), carbon dioxide Cape Grim data courtesy of Paul Krummel and Paul
29 Steele, CSIRO, and CGBAPS. Benzene and acetylene data from GCMS analysis of NOAA
30 HATS flasks collected at Cape Grim courtesy of Steve Montzka, (NOAA). OH concentration
31 data from Cape Grim provided by Stephen Wilson (University of Wollongong). Chatham

1 Rise carbon dioxide data provided by John McGregor (NIWA) and chlorophyll-*a* data
2 provided by Cliff Law (NIWA).
3 Sarah Lawson would like to acknowledge the NIWA Visiting Scientist Scheme and CSIRO's
4 Capability Development Fund for providing financial support for her participation in the
5 SOAP voyage.

6

7 **References**

8 Ayers, G. P., and Gras, J. L.: Seasonal relationship between cloud condensation nuclei and
9 aerosol methanesulfonate in marine air *Nature*, 353, 834-835, 1991.

10 Bates, T. S., Quinn, P. K., Frossard, A. A., Russell, L. M., Hakala, J., Petäjä, T., Kulmala, M.,
11 Covert, D. S., Cappa, C. D., Li, S. M., Hayden, K. L., Nuaaman, I., McLaren, R., Massoli, P.,
12 Canagaratna, M. R., Onasch, T. B., Sueper, D., Worsnop, D. R., and Keene, W. C.:
13 Measurements of ocean derived aerosol off the coast of California, *Journal of Geophysical
14 Research: Atmospheres*, 117, D00V15, 10.1029/2012JD017588, 2012.

15 Betterton, E. A., and Hoffmann, M. R.: Henry's law constants of some environmentally
16 important aldehydes, *Environmental Science & Technology*, 22, 1415-1418,
17 10.1021/es00177a004, 1988.

18 Bikkina, S., Kawamura, K., Miyazaki, Y., and Fu, P.: High abundances of oxalic, azelaic, and
19 glyoxylic acids and methylglyoxal in the open ocean with high biological activity:
20 Implication for secondary OA formation from isoprene, *Geophysical Research Letters*, 41,
21 2014GL059913, 10.1002/2014GL059913, 2014.

22 Bowie, A. R., Brian Griffiths, F., Dehairs, F., and Trull, T. W.: Oceanography of the
23 subantarctic and Polar Frontal Zones south of Australia during summer: Setting for the SAZ-
24 Sense study, *Deep Sea Research Part II: Topical Studies in Oceanography*, 58, 2059-2070,
25 <http://dx.doi.org/10.1016/j.dsr2.2011.05.033>, 2011.

26 Carslaw, K. S., Lee, L. A., Reddington, C. L., Pringle, K. J., Rap, A., Forster, P. M., Mann,
27 G. W., Spracklen, D. V., Woodhouse, M. T., Regayre, L. A., and Pierce, J. R.: Large
28 contribution of natural aerosols to uncertainty in indirect forcing, *Nature*, 503, 67-+,
29 10.1038/nature12674, 2013.

30 Claeys, M., Wang, W., Vermeylen, R., Kourtchev, I., Chi, X. G., Farhat, Y., Surratt, J. D.,
31 Gomez-Gonzalez, Y., Sciare, J., and Maenhaut, W.: Chemical characterisation of marine
32 aerosol at Amsterdam Island during the austral summer of 2006-2007, *J. Aerosol. Sci.*, 41,
33 13-22, 10.1016/j.jaerosci.2009.08.003, 2010.

34 Coburn, S., Ortega, I., Thalman, R., Blomquist, B., Fairall, C. W., and Volkamer, R.:
35 Measurements of diurnal variations and Eddy Covariance (EC) fluxes of glyoxal in the
36 tropical marine boundary layer: description of the Fast LED-CE-DOAS instrument, *Atmos.
37 Meas. Tech. Discuss.*, 7, 6245-6285, 10.5194/amt-7-6245-2014, 2014.

38 Decesari, S., Finessi, E., Rinaldi, M., Paglione, M., Fuzzi, S., Stephanou, E. G., Tziaras, T.,
39 Spyros, A., Ceburnis, D., O'Dowd, C., Dall'Osto, M., Harrison, R. M., Allan, J., Coe, H., and
40 Facchini, M. C.: Primary and secondary marine organic aerosols over the North Atlantic

1 Ocean during the MAP experiment, *Journal of Geophysical Research-Atmospheres*, 116, 21,
2 D22210 10.1029/2011jd016204, 2011.

3 Donahue, N. M., Robinson, A. L., Trump, E. R., Riipinen, I., and Kroll, J. H.: Volatility and
4 Aging of Atmospheric Organic Aerosol, in: *Atmospheric and Aerosol Chemistry*, edited by:
5 McNeill, V. F., and Ariya, P. A., *Topics in Current Chemistry*, 97-143, 2014.

6 Ervens, B., Turpin, B. J., and Weber, R. J.: Secondary organic aerosol formation in cloud
7 droplets and aqueous particles (aqSOA): a review of laboratory, field and model studies,
8 *Atmospheric Chemistry and Physics*, 11, 11069-11102, 10.5194/acp-11-11069-2011, 2011.

9 Facchini, M. C., Decesari, S., Rinaldi, M., Carbone, C., Finessi, E., Mircea, M., Fuzzi, S.,
10 Moretti, F., Tagliavini, E., Ceburnis, D., and O'Dowd, C. D.: Important Source of Marine
11 Secondary Organic Aerosol from Biogenic Amines, *Environmental Science & Technology*,
12 42, 9116-9121, 10.1021/es8018385, 2008a.

13 Facchini, M. C., Rinaldi, M., Decesari, S., Carbone, C., Finessi, E., Mircea, M., Fuzzi, S.,
14 Ceburnis, D., Flanagan, R., Nilsson, E. D., de Leeuw, G., Martino, M., Woeltjen, J., and
15 O'Dowd, C. D.: Primary submicron marine aerosol dominated by insoluble organic colloids
16 and aggregates, *Geophysical Research Letters*, 35, L17814, 10.1029/2008GL034210, 2008b.

17 Fu, P. Q., Kawamura, K., and Miura, K.: Molecular characterization of marine organic
18 aerosols collected during a round-the-world cruise, *Journal of Geophysical Research-
Atmospheres*, 116, 14, D13302 10.1029/2011jd015604, 2011.

20 Fu, P. Q., Kawamura, K., Chen, J., Charriere, B., and Sempere, R.: Organic molecular
21 composition of marine aerosols over the Arctic Ocean in summer: contributions of primary
22 emission and secondary aerosol formation, *Biogeosciences*, 10, 653-667, 10.5194/bg-10-653-
23 2013, 2013.

24 Fu, T. M., Jacob, D. J., Wittrock, F., Burrows, J. P., Vrekoussis, M., and Henze, D. K.:
25 Global budgets of atmospheric glyoxal and methylglyoxal, and implications for formation of
26 secondary organic aerosols, *Journal of Geophysical Research-Atmospheres*, 113, D15303
27 10.1029/2007jd009505, 2008.

28 Galbally, I. E., Lawson, S. J., Weeks, I. A., Bentley, S. T., Gillett, R. W., Meyer, M., and
29 Goldstein, A. H.: Volatile organic compounds in marine air at Cape Grim, Australia,
30 *Environmental Chemistry*, 4, 178-182, 10.1071/en07024, 2007.

31 Gras, J. L.: Postfrontal nanoparticles at Cape Grim: impact on cloud nuclei concentrations,
32 *Environmental Chemistry*, 6, 515-523, 10.1071/en09076, 2009.

33 Gras, J. L.: Particles Program Report, Baseline Atmospheric Program (Australia) 2009-2010,
34 edited by: Derek, N., and Krummel, P. B., and Cleland, S.J., Australian Bureau of
35 Meteorology and CSIRO Marine and Atmospheric Research, Melbourne, 73-75, 2014.
36 http://www.bom.gov.au/inside/cgbaps/baseline/Baseline_2009-2010.pdf

37 Grutter, M., Flores, E., Andracia-Ayala, G., and Báez, A.: Formaldehyde levels in downtown
38 Mexico City during 2003, *Atmospheric Environment*, 39, 1027-1034,
39 <http://dx.doi.org/10.1016/j.atmosenv.2004.10.031>, 2005.

40 Helmg, D., Bottenheim, J., Galbally, I. E., Lewis, A., Milton, M. J. T., Penkett, S., Plass-
41 Duelmer, C., Reimann, S., Tans, P., and Thiel, S.: Volatile Organic Compounds in the Global
42 Atmosphere, *Eos, Transactions American Geophysical Union*, 90, 513-514,
43 10.1029/2009EO520001, 2009.

1 Helmig, D., Petrenko, V., Martinerie, P., Witrant, E., Röckmann, T., Zuiderweg, A.,
2 Holzinger, R., Hueber, J., Thompson, C., White, J. W. C., Sturges, W., Baker, A., Blunier, T.,
3 Etheridge, D., Rubino, M., and Tans, P.: Reconstruction of Northern Hemisphere
4 1950–2010 atmospheric non-methane hydrocarbons, *Atmos. Chem. Phys.*, 14, 1463–
5 1483, 10.5194/acp-14-1463-2014, 2014.

6 ISO: ISO 6879: Air Quality, Performance Characteristics and Related Concepts for Air
7 Quality Measuring Methods, International Organisation for Standardisation Geneva,
8 Switzerland 1995.

9 Kampf, C. J., Waxman, E. M., Slowik, J. G., Dommen, J., Pfaffenberger, L., Praplan, A. P.,
10 Prevot, A. S. H., Baltensperger, U., Hoffmann, T., and Volkamer, R.: Effective Henry's Law
11 Partitioning and the Salting Constant of Glyoxal in Aerosols Containing Sulfate, *Environ.*
12 *Sci. Technol.*, 47, 4236–4244, 10.1021/es400083d, 2013.

13 Keywood, M. D.: Aerosol composition at Cape Grim : an evaluation of PM10 sampling
14 program and baseline event switches, in: Baseline Atmospheric Program Australia 2005–
15 2006, edited by: Cainey, J. M., Derek, N., and Krummel, P. B., Australian Bureau of
16 Meteorology and CSIRO Marine and Atmospheric Research, Melbourne, 31–36, 2007.
17 http://www.bom.gov.au/inside/cgbaps/baseline/Baseline_2005-2006.pdf

18 Kivlighon, L. M.: Tropospheric non-methane hydrocarbons at Cape Grim. Masters Thesis,
19 Department of Chemistry, La Trobe University, Melbourne, Australia 2001.

20 Korhonen, H., Carslaw, K. S., Spracklen, D. V., Mann, G. W., and Woodhouse, M. T.:
21 Influence of oceanic dimethyl sulfide emissions on cloud condensation nuclei concentrations
22 and seasonality over the remote Southern Hemisphere oceans: A global model study, *Journal*
23 *of Geophysical Research-Atmospheres*, 113, D15204 10.1029/2007jd009718, 2008.

24 Kroll, J. H., Ng, N. L., Murphy, S. M., Varutbangkul, V., Flagan, R. C., and Seinfeld, J. H.:
25 Chamber studies of secondary organic aerosol growth by reactive uptake of simple carbonyl
26 compounds, *Journal of Geophysical Research-Atmospheres*, 110, D23207
27 10.1029/2005jd006004, 2005.

28 Kwan, A. J., Crounse, J. D., Clarke, A. D., Shinozuka, Y., Anderson, B. E., Crawford, J. H.,
29 Avery, M. A., McNaughton, C. S., Brune, W. H., Singh, H. B., and Wennberg, P. O.: On the
30 flux of oxygenated volatile organic compounds from organic aerosol oxidation, *Geophysical*
31 *Research Letters*, 33, 10.1029/2006gl026144, 2006.

32 Lana, A., Simo, R., Vallina, S. M., and Dachs, J.: Potential for a biogenic influence on cloud
33 microphysics over the ocean: a correlation study with satellite-derived data, *Atmospheric*
34 *Chemistry and Physics*, 12, 7977–7993, 10.5194/acp-12-7977-2012, 2012.

35 Landwehr, S., Miller, S. D., Smith, M. J., Saltzman, E. S., and Ward, B.: Analysis of the PKT
36 correction for direct CO₂ flux measurements over the ocean, *Atmos. Chem. Phys.*, 14, 3361–
37 3372, 10.5194/acp-14-3361-2014, 2014.

38 Lawson, S. J., Galbally, I. E., Gras, J. L., and Dunne, E.: Measurement of VOCs in Marine
39 Air at Cape Grim using PTR-MS, Baseline Atmospheric Program 2007–2008, edited by:
40 Derek, N., and Krummel, P. B., Australian Bureau of Meteorology and CSIRO Marine and
41 Atmospheric Research, Melbourne 2011.
42 http://www.bom.gov.au/inside/cgbaps/baseline/Baseline_2007-2008.pdf

43 Lee, A. K. Y., Herckes, P., Leaitch, W. R., Macdonald, A. M., and Abbatt, J. P. D.: Aqueous
44 OH oxidation of ambient organic aerosol and cloud water organics: Formation of highly

1 oxidized products, *Geophysical Research Letters*, 38, 5, L11805 10.1029/2011gl047439,
2 2011.

3 Lerot, C., Stavrakou, T., De Smedt, I., Muller, J. F., and Van Roozendael, M.: Glyoxal
4 vertical columns from GOME-2 backscattered light measurements and comparisons with a
5 global model, *Atmospheric Chemistry and Physics*, 10, 12059-12072, 10.5194/acp-10-12059-
6 2010, 2010.

7 Lim, Y. B., Tan, Y., and Turpin, B. J.: Chemical insights, explicit chemistry, and yields of
8 secondary organic aerosol from OH radical oxidation of methylglyoxal and glyoxal in the
9 aqueous phase, *Atmospheric Chemistry and Physics*, 13, 8651-8667, 10.5194/acp-13-8651-
10 2013, 2013.

11 Mahajan, A. S., Prados-Roman, C., Hay, T. D., Lampel, J., Pöhler, D., Großmann, K.,
12 Tschritter, J., Frieß, U., Platt, U., Johnston, P., Kreher, K., Wittrock, F., Burrows, J. P., Plane,
13 J. M. C., and Saiz-Lopez, A.: Glyoxal observations in the global marine boundary layer,
14 *Journal of Geophysical Research: Atmospheres*, 119, 2013JD021388,
15 10.1002/2013JD021388, 2014.

16 Meskhidze, N., and Nenes, A.: Phytoplankton and cloudiness in the Southern Ocean, *Science*,
17 314, 1419-1423, 10.1126/science.1131779, 2006.

18 Meskhidze, N., Xu, J., Gantt, B., Zhang, Y., Nenes, A., Ghan, S. J., Liu, X., Easter, R., and
19 Zaveri, R.: Global distribution and climate forcing of marine organic aerosol: 1. Model
20 improvements and evaluation, *Atmospheric Chemistry and Physics*, 11, 11689-11705,
21 10.5194/acp-11-11689-2011, 2011.

22 Miller, C. C., Abad, G. G., Wang, H., Liu, X., Kurosu, T., Jacob, D. J., and Chance, K.:
23 Glyoxal retrieval from the Ozone Monitoring Instrument, *Atmos. Meas. Tech. Discuss.*, 7,
24 6065-6112, 10.5194/amtd-7-6065-2014, 2014.

25 Molloy, S. B., and Galbally, I. E.: Analysis and identification of a suitable Baseline definition
26 for tropospheric ozone at Cape Grim, Tasmania, *Baseline Atmospheric Program (Australia)*
27 2009-2010 edited by: Derek, N., and Krummel, P. B., and Cleland, S.J., Australian Bureau of
28 Meteorology and CSIRO Marine and Atmospheric Research, Melbourne, 7-16, 2014.
29 http://www.bom.gov.au/inside/cgbaps/baseline/Baseline_2009-2010.pdf

30 Montzka, S. A., Siso, C., Mondeel, D., Miller, B. R., Hall, B., Elkins, J. W., and Butler, J. H.:
31 Flask Measurements at Cape Grim Baseline Air Pollution Station by the HATS group of
32 NOAA/ESRL/GMD, *Baseline Atmospheric Program (Australia)* 2009-2010, 2014.

33 Muller, K., Lehmann, S., van Pinxteren, D., Gnauk, T., Niedermeier, N., Wiedensohler, A.,
34 and Herrmann, H.: Particle characterization at the Cape Verde atmospheric observatory
35 during the 2007 RHaMBLe intensive, *Atmospheric Chemistry and Physics*, 10, 2709-2721,
36 2010.

37 Myrookefalitakis, S., Vrekoussis, M., Tsigaridis, K., Wittrock, F., Richter, A., Brühl, C.,
38 Volkamer, R., Burrows, J. P., and Kanakidou, M.: The influence of natural and anthropogenic
39 secondary sources on the glyoxal global distribution, *Atmos. Chem. Phys.*, 8, 4965-4981,
40 10.5194/acp-8-4965-2008, 2008.

41 O'Dowd, C. D., Facchini, M. C., Cavalli, F., Ceburnis, D., Mircea, M., Decesari, S., Fuzzi, S.,
42 Yoon, Y. J., and Putaud, J. P.: Biogenically driven organic contribution to marine aerosol,
43 *Nature*, 431, 676-680, 10.1038/nature02959, 2004.

44 Olsen, R., Thorud, S., Hersson, M., Ovrebo, S., Lundanes, E., Greibrokk, T., Ellingsen, D.
45 G., Thomassen, Y., and Molander, P.: Determination of the dialdehyde glyoxal in workroom

1 air-development of personal sampling methodology, *Journal of Environmental Monitoring*, 9,
2 687-694, 10.1039/B700105N, 2007.

3 Orellana, M. V., Matrai, P. A., Leck, C., Rauschenberg, C. D., Lee, A. M., and Coz, E.:
4 Marine microgels as a source of cloud condensation nuclei in the high Arctic, *Proceedings of*
5 the National Academy of Sciences, 108, 13612-13617, 10.1073/pnas.1102457108, 2011.

6 Ovadnevaite, J., Ceburnis, D., Martucci, G., Bialek, J., Monahan, C., Rinaldi, M., Facchini,
7 M. C., Berresheim, H., Worsnop, D. R., and O'Dowd, C.: Primary marine organic aerosol: A
8 dichotomy of low hygroscopicity and high CCN activity, *Geophysical Research Letters*, 38,
9 5, L21806 10.1029/2011gl048869, 2011a.

10 Ovadnevaite, J., O'Dowd, C., Dall'Osto, M., Ceburnis, D., Worsnop, D. R., and Berresheim,
11 H.: Detecting high contributions of primary organic matter to marine aerosol: A case study,
12 *Geophysical Research Letters*, 38, 5, L02807 10.1029/2010gl046083, 2011b.

13 Pétron, G., Frost, G., Miller, B. R., Hirsch, A. I., Montzka, S. A., Karion, A., Trainer, M.,
14 Sweeney, C., Andrews, A. E., Miller, L., Kofler, J., Bar-Ilan, A., Dlugokencky, E. J., Patrick,
15 L., Moore, C. T., Ryerson, T. B., Siso, C., Kolodzey, W., Lang, P. M., Conway, T., Novelli,
16 P., Masarie, K., Hall, B., Guenther, D., Kitzis, D., Miller, J., Welsh, D., Wolfe, D., Neff, W.,
17 and Tans, P.: Hydrocarbon emissions characterization in the Colorado Front Range: A pilot
18 study, *Journal of Geophysical Research: Atmospheres*, 117, D04304,
19 10.1029/2011JD016360, 2012.

20 Rhoderick, G. C., Duewer, D. L., Apel, E., Baldan, A., Hall, B., Harling, A., Helmig, D.,
21 Heo, G. S., Hueber, J., Kim, M. E., Kim, Y. D., Miller, B., Montzka, S., and Riemer, D.:
22 International Comparison of a Hydrocarbon Gas Standard at the Picomol per Mol Level,
23 *Analytical Chemistry*, 86, 2580-2589, 10.1021/ac403761u, 2014.

24 Rinaldi, M., Decesari, S., Finessi, E., Julianelli, L., Carbone, C., Fuzzi, S., O'Dowd, C.,
25 Ceburnis, D., and Facchini, M. C.: Primary and Secondary Organic Marine Aerosol and
26 Oceanic Biological Activity: Recent Results and New Perspectives for Future Studies,
27 *Advances in Meteorology*, 2010, 10.1155/2010/310682, 2010.

28 Rinaldi, M., Decesari, S., Carbone, C., Finessi, E., Fuzzi, S., Ceburnis, D., O'Dowd, C. D.,
29 Sciare, J., Burrows, J. P., Vrekoussis, M., Ervens, B., Tsigaridis, K., and Facchini, M. C.:
30 Evidence of a natural marine source of oxalic acid and a possible link to glyoxal, *Journal of*
31 *Geophysical Research-Atmospheres*, 116, 12, D16204 10.1029/2011jd015659, 2011.

32 Schauer, J. J., Kleeman, M. J., Cass, G. R., and Simoneit, B. R. T.: Measurement of
33 Emissions from Air Pollution Sources. 2. C1 through C30 Organic Compounds from Medium
34 Duty Diesel Trucks, *Environ. Sci. Technol.*, 33, 1578-1587, 10.1021/es980081n, 1999.

35 Sciare, J., Favez, O., Sarda-Esteve, R., Oikonomou, K., Cachier, H., and Kazan, V.: Long-
36 term observations of carbonaceous aerosols in the Austral Ocean atmosphere: Evidence of a
37 biogenic marine organic source, *Journal of Geophysical Research-Atmospheres*, 114, D15302
38 10.1029/2009jd011998, 2009.

39 Sedehi, N., Takano, H., Blasic, V. A., Sullivan, K. A., and De Haan, D. O.: Temperature- and
40 pH-dependent aqueous-phase kinetics of the reactions of glyoxal and methylglyoxal with
41 atmospheric amines and ammonium sulfate, *Atmos. Environ.*, 77, 656-663,
42 10.1016/j.atmosenv.2013.05.070, 2013.

43 Shaw, S., Gantt, B., and Meskhidze, N.: Production and Emission of Marine Isoprene and
44 Monoterpenes: a review, *Advances in Meteorology*, 2010, 10.1155/2010/408696, 2010.

1 Sinreich, R., Volkamer, R., Filsinger, F., Frieß, U., Kern, C., Platt, U., Sebastián, O., and
2 Wagner, T.: MAX-DOAS detection of glyoxal during ICARTT 2004, *Atmos. Chem. Phys.*,
3 7, 1293-1303, 10.5194/acp-7-1293-2007, 2007.

4 Sinreich, R., Coburn, S., Dix, B., and Volkamer, R.: Ship-based detection of glyoxal over the
5 remote tropical Pacific Ocean, *Atmospheric Chemistry and Physics*, 10, 11359-11371,
6 10.5194/acp-10-11359-2010, 2010.

7 Slemr, J.: Determination of volatile carbonyl compounds in clean air, *Fresenius J Anal Chem.*,
8 340, 672-677, 10.1007/BF00321533, 1991.

9 Sommariva, R., Haggerstone, A. L., Carpenter, L. J., Carslaw, N., Creasey, D. J., Heard, D.
10 E., Lee, J. D., Lewis, A. C., Pilling, M. J., and Zádor, J.: OH and HO₂ chemistry in clean
11 marine air during SOAPEX-2, *Atmos. Chem. Phys.*, 4, 839-856, 10.5194/acp-4-839-2004,
12 2004.

13 Stavrakou, T., Müller, J. F., De Smedt, I., Van Roozendael, M., Kanakidou, M., Vrekoussis,
14 M., Wittrock, F., Richter, A., and Burrows, J. P.: The continental source of glyoxal estimated
15 by the synergistic use of spaceborne measurements and inverse modelling, *Atmos. Chem.*
16 *Phys.*, 9, 8431-8446, 10.5194/acp-9-8431-2009, 2009.

17 Steele, P., Krummel, P., van der Schoot, M. V., Spencer, D. A., Baly, S. B., Langenfelds, R.
18 L., Howden, R. T., Ward, J., Somerville, N. T., and Cleland, S. J.: Baseline carbon dioxide
19 monitoring, *Baseline Atmospheric Program (Australia) 2009-2010*, edited by: Derek, N., and
20 Krummel, P. B., and Cleland, S.J., Australian Bureau of Meteorology and CSIRO Marine and
21 Atmospheric Research, Melbourne, 39-41, 2014.
22 http://www.bom.gov.au/inside/cgbaps/baseline/Baseline_2009-2010.pdf

23 Tan, Y., Lim, Y. B., Altieri, K. E., Seitzinger, S. P., and Turpin, B. J.: Mechanisms leading to
24 oligomers and SOA through aqueous photooxidation: insights from OH radical oxidation of
25 acetic acid and methylglyoxal, *Atmospheric Chemistry and Physics*, 12, 801-813,
26 10.5194/acp-12-801-2012, 2012.

27 Thalman, R., Baeza-Romera, M. T., Ball, S. M., Borras, E., Daniels, M. J. S., Goodall, I. C.
28 A., Henry, S. B., Karl, T., Keutsch, F. N., Kim, S., Mak, J., Monks, P. S., Munoz, A.,
29 Orlando, J. J., Peppe, S., Rickard, A. R., Rodenas, M., Sanchez, P., Seco, R., Su, L., Tyndall,
30 G., Vazquez, M., Vera, T., Waxman, E., and Volkamer, R.: Instrument Inter-comparison of
31 glyoxal, methyl glyoxal and NO₂ under simulated atmospheric conditions, *Atmospheric*
32 *Measurement Techniques Discussions*, In press, 2014.

33 Topping, D., Connolly, P., and McFiggans, G.: Cloud droplet number enhanced by co-
34 condensation of organic vapours, *Nature Geosci.*, 6, 443-446, 10.1038/ngeo1809
35 <http://www.nature.com/ngeo/journal/v6/n6/abs/ngeo1809.html#supplementary-information>,
36 2013.

37 van Pinxteren, M., and Herrmann, H.: Glyoxal and methylglyoxal in Atlantic seawater and
38 marine aerosol particles: method development and first application during the Polarstern
39 cruise ANT XXVII/4, *Atmospheric Chemistry and Physics*, 13, 11791-11802, 10.5194/acp-
40 13-11791-2013, 2013.

41 Volkamer, R.: Measurements of Bromine Oxide, Iodine Oxide and Oxygenated
42 Hydrocarbons in the Tropical Free Troposphere from Research Aircraft and Mountaintops,
43 NOAA ESRL Global Monitoring Annual Conference 2014, Boulder, Colorado, 2014.

1 Vrekoussis, M., Wittrock, F., Richter, A., and Burrows, J. P.: Temporal and spatial variability
2 of glyoxal as observed from space, *Atmospheric Chemistry and Physics*, 9, 4485-4504,
3 10.5194/acp-9-4485-2009, 2009.

4 Wang, H.-L., Zhang, X., and Chen, Z.-M.: Development of DNPH/HPLC method for the
5 measurement of carbonyl compounds in the aqueous phase: applications to laboratory
6 simulation and field measurement, *Environ. Chem.*, 6, 389-397,
7 <http://dx.doi.org/10.1071/EN09057>, 2009.

8 Westervelt, D. M., Moore, R. H., Nenes, A., and Adams, P. J.: Effect of primary organic sea
9 spray emissions on cloud condensation nuclei concentrations, *Atmospheric Chemistry and*
10 *Physics*, 12, 89-101, 10.5194/acp-12-89-2012, 2012.

11 Wilson, S. R.: Characterisation of J(O1D) at Cape Grim 2000–2005, *Atmos. Chem. Phys.*
12 *Discuss.*, 14, 18389-18419, 10.5194/acpd-14-18389-2014, 2014.

13 Wittrock, F., Richter, A., Oetjen, H., Burrows, J. P., Kanakidou, M., Myriokefalitakis, S.,
14 Volkamer, R., Beirle, S., Platt, U., and Wagner, T.: Simultaneous global observations of
15 glyoxal and formaldehyde from space, *Geophys. Res. Lett.*, 33, 10.1029/2006gl026310,
16 2006.

17 Zahorowski, W., Griffiths, A. D., Chambers, S. D., Williams, A. G., Law, R. M., Crawford,
18 J., and Werczynski, S.: Constraining annual and seasonal radon-222 flux density from the
19 Southern Ocean using radon-222 concentrations in the boundary layer at Cape Grim, *Tellus*
20 B, 65, 2013.

21 Zhou, S., Gonzalez, L., Leithead, A., Finewax, Z., Thalman, R., Vlasenko, A., Vagle, S.,
22 Miller, L. A., Li, S. M., Bureekul, S., Furutani, H., Uematsu, M., Volkamer, R., and Abbatt,
23 J.: Formation of gas-phase carbonyls from heterogeneous oxidation of polyunsaturated fatty
24 acids at the air–water interface and of the sea surface microlayer, *Atmos. Chem. Phys.*, 14,
25 1371-1384, 10.5194/acp-14-1371-2014, 2014.

26 Zhou, X., and Mopper, K.: Apparent partition coefficients of 15 carbonyl compounds
27 between air and seawater and between air and freshwater; implications for air-sea exchange,
28 *Environ. Sci. Technol.*, 24, 1864-1869, 10.1021/es00082a013, 1990.

29

30

31

1 Tab01

2

Site	Season	Glyoxal (ppt)	Methylglyoxal (ppt)	CO ₂ (ppm)	CN>10nm (particles cm ⁻³)	Radon (mBq m ⁻³)	% Baseline hours
Cape Grim n=5	Winter/Spring (Aug-Sep)	7 ± 2	28 ± 11	388.84 ± 0.12	194 ± 110	43± 14	95
SOAP voyage n=2	Summer (Feb- Mar)	23 ± 8	10 ± 10	388.54 ± 0.82	328 ± 1591	n/a	n/a

Temperate ocean

Tropical ocean

	Southern Ocean (Cape Grim)	South West Pacific (Chatham Rise)	South West Pacific (Chatham Rise) ^a	North Pacific & Atlantic ^a	Tropical Pacific & Atlantic ^a	Eastern Tropical Pacific ^b	Tropical Pacific ^c	Caribbean and Sargasso Sea ^d
Glyoxal	Clean marine origin	7 ± 2	23 ± 8	-	-	-	43 ± 9 (SH) 32 ± 6 (NH)	63 ± 21
	All data	10 ± 6	30 ± 12	23 ± 10	25 ± 13	24 ± 12 (SH) 26 ± 15 (NH)	-	80
Methyl-glyoxal	Clean marine origin	28 ± 11	10 ± 10	-	-	-	-	-
	All data	57 ± 32	19 ± 14	-	-	-	-	~10

1 Tab03

Precursor	precursor mixing ratios (ppt)		glyoxal yield (ppt)		methylglyoxal yield (ppt)	
	Chatham Rise	Cape Grim	Chatham Rise	Cape Grim	Chatham Rise	Cape Grim
acetylene	3 ^a	39 ^a	0.02	0.08	n/a	n/a
ethene	51 ^b	31 ^b	0.22	0.06	n/a	n/a
propene	17 ^b	8 ^b	n/a	n/a	0.04	0.03
propane	33 ^c	35 ^c	n/a	n/a	0.02	0.02
alkanes >C ₃ [^]	54	52 ^c	n/a	n/a	0.02	0.02
isoprene	14	14 ^d	0.85	0.43	1.89	1.97
benzene	8	9 ^a	0.02	0.01	n/a	n/a
toluene	9	9 [*]	0.08	0.03	0.03	0.03
xylenes sum	10	9 [*]	0.27	0.10	0.22	0.19
monoterpenes	32	17 ^e	0.83	0.44	0.69	0.48
acetone	89	118 ^d	n/a	n/a	0.01	0.02
sum yield (ppt)			2.3	1.2	2.9	2.8
% explained			10	17	29	10

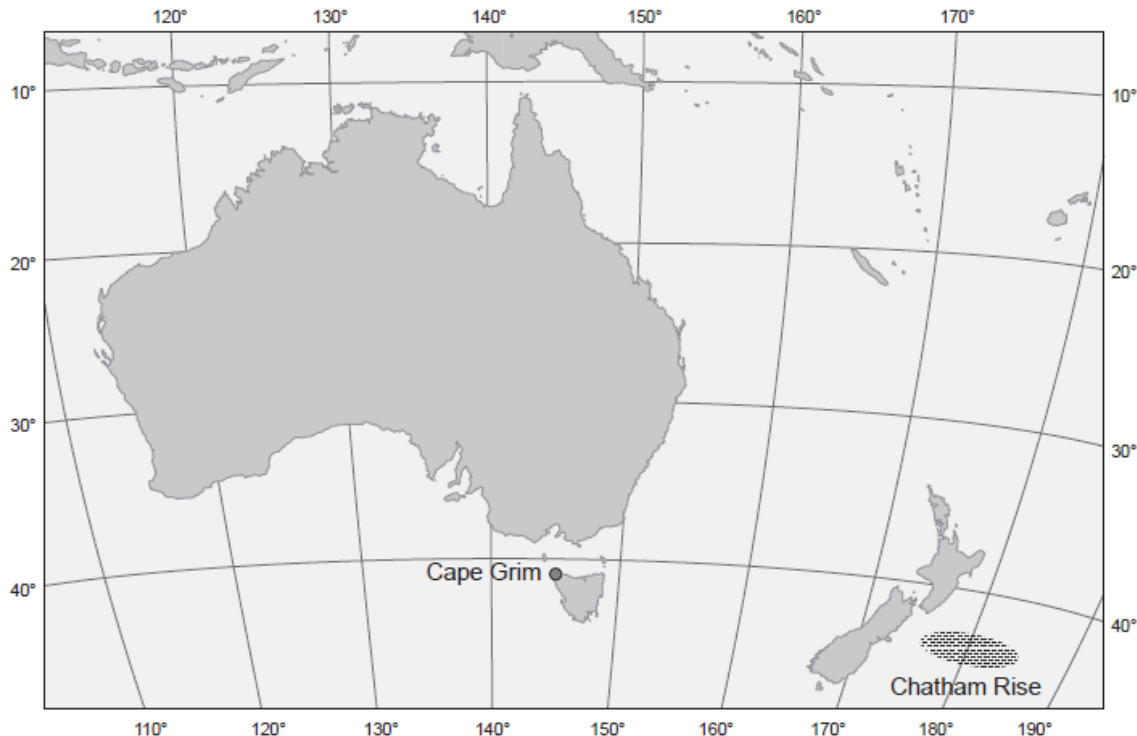
2

1 Table 1. Mixing ratios of glyoxal and methylglyoxal in clean marine air at Cape Grim and
2 Chatham Rise, with supporting measurements of carbon dioxide, condensation nuclei (CN)
3 >10nm and atmospheric radon-222. Values are average \pm std dev. n = number of 24 hour
4 samples.

5 Table 2. Glyoxal and methylglyoxal compared to dicarbonyl measurements from other
6 remote oceanic sites. Data is listed as clean marine origin where study explicitly excludes
7 terrestrial influence. All concs are in ppt. Values are mean \pm std dev SH= Southern
8 Hemisphere, NH= Northern Hemisphere. ^a Mahajan et al. 2014 (only data above MDL has
9 been included in average) ^b Coburn et al. 2014 ^c Sinreich et al. 2010 ^d Zhou and Mopper 1990
10 Table 3. Calculated dicarbonyl yields based on precursor data from Cape Grim and Chatham
11 Rise. Yields and dicarbonyl lifetimes based on Fu et al. (2008). Where supplementary (e.g.
12 non-parallel) measurements were used these are denoted as follows: ^aCape Grim flasks
13 (NOAA HATS analysis) ^bKivlighon 2001 ^cCape Grim flasks (INSTAAR analysis) ^dGalbally
14 et al. 2007 (upper estimate Cape Grim summer) ^eLawson et al. 2011 (Cape Grim Baseline
15 spring data, see text for explanation) [^] sum of C₄ and C₅ ^{*}upper estimate based on benzene

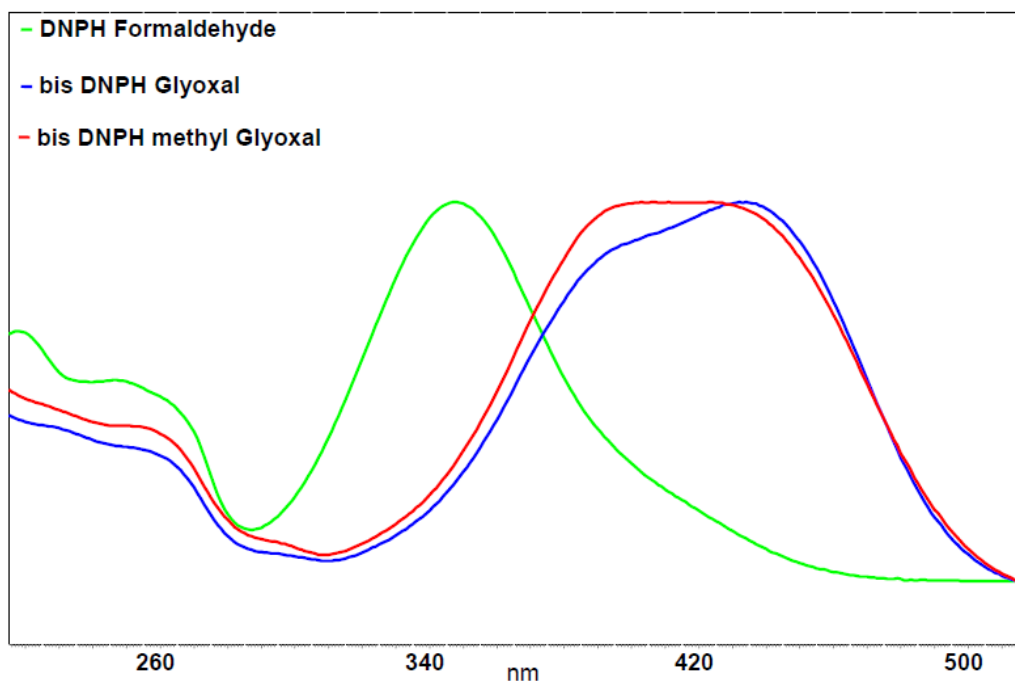
16

17 Figure 1. Cape Grim and Chatham Rise sampling locations

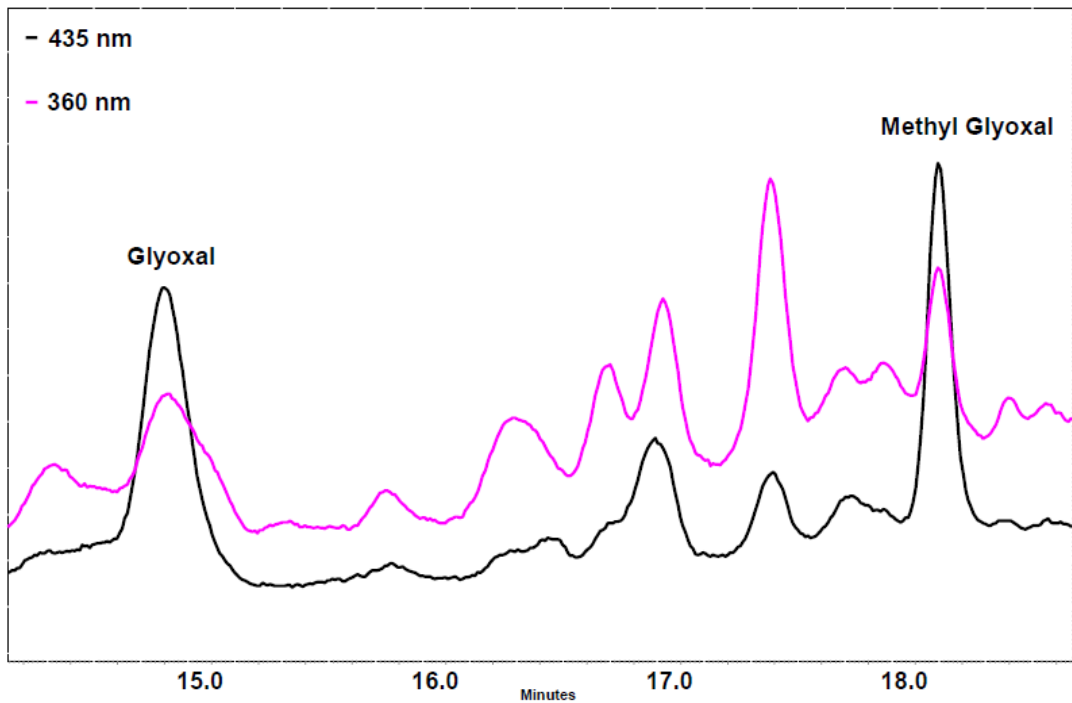


18

1 Figure 2. Absortion spectra for monocarbonyl formaldehyde (green) and dicarbonyls glyoxal
2 (blue line) and methylglyoxal (red line)

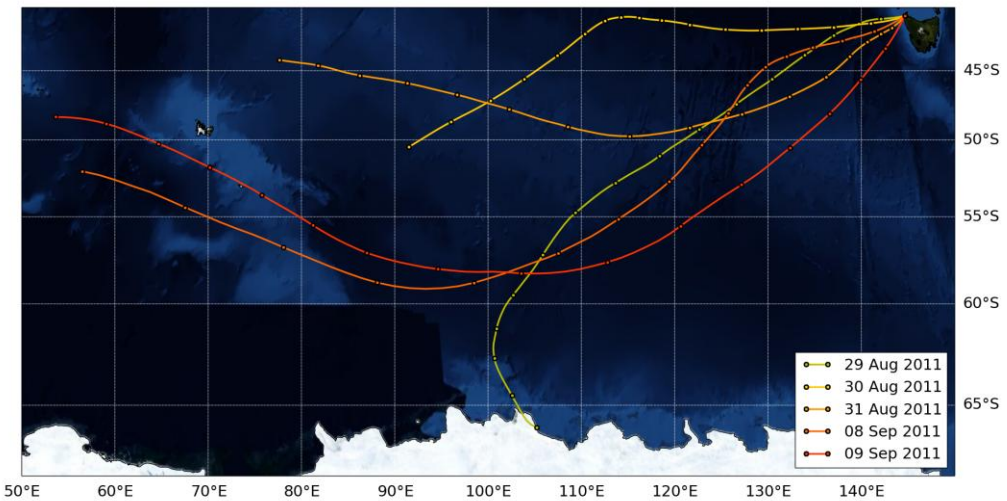


3
4 Figure 3. Example of sample chromatogram from Chatham Rise using absorption at 360nm
5 (pink line) and 435nm (black line).



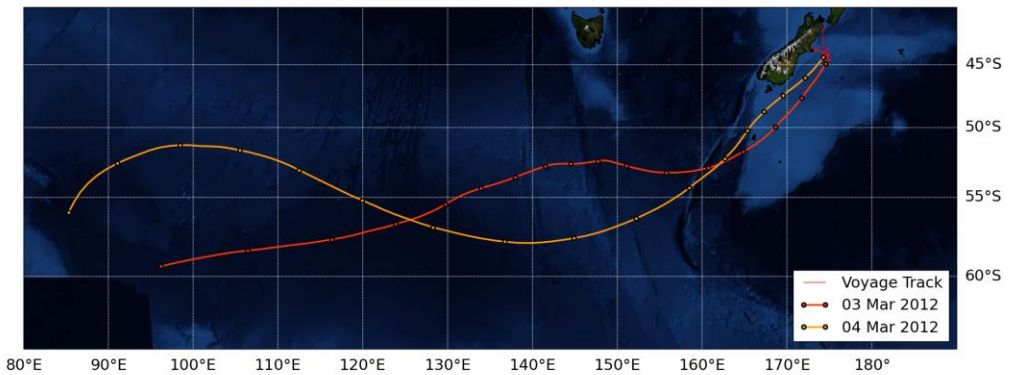
1

2 Figure 4a. HYSPLIT 96 hour back trajectory for the 5 clean marine samples from Cape Grim



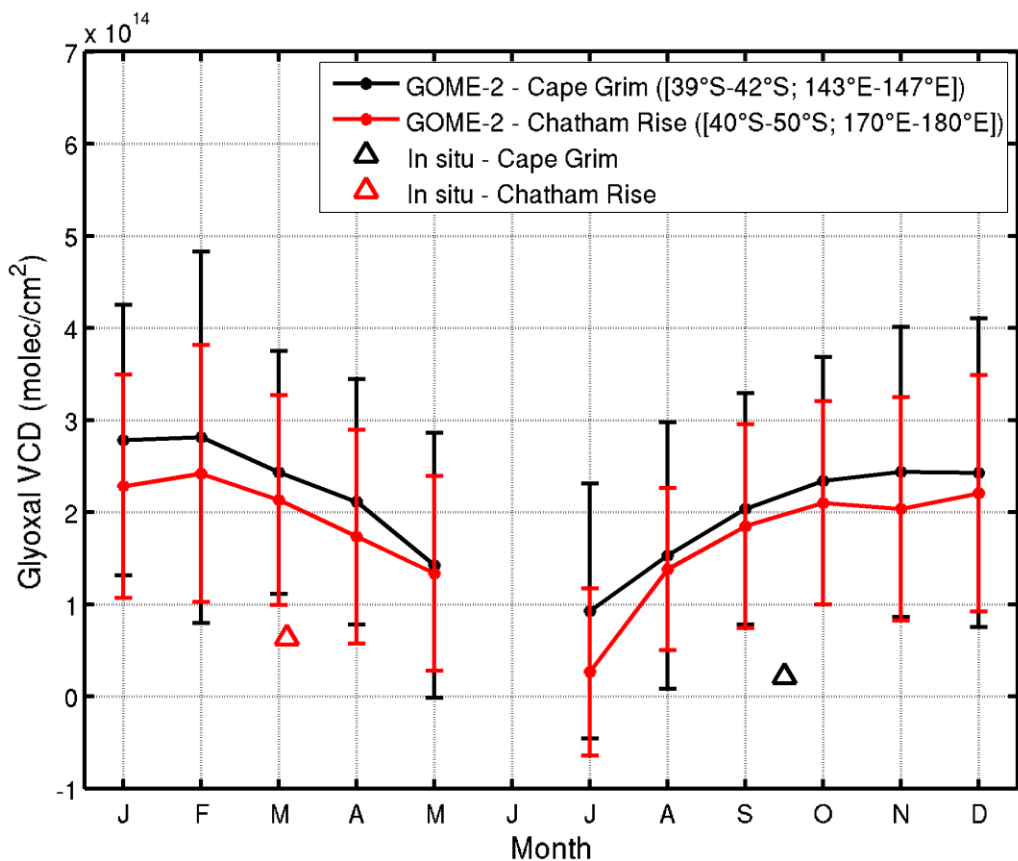
3

4 Figure 4b. HYSPLIT 96 hour back trajectory for the 2 clean marine samples from the SOAP
5 Voyage (Chatham Rise)



1

2 Figure 5. Seasonal glyoxal VCDs retrieved from GOME-2 and calculated from surface based
 3 observations at Cape Grim and Chatham Rise. GOME-2 values are for all data averaged
 4 between 2007-2012, for regions encompassing Cape Grim and Chatham Rise. Error bars for
 5 surface-based VCDs are insignificant on this scale and are not shown (see text for details).



6

1

2

3

4